Geothermics 139 (2026) 103658

Contents lists available at ScienceDirect

Geothermics

journal homepage: www.elsevier.com/locate/geothermics

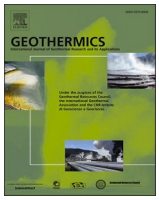

Thermal performance testing of shallow geothermal systems: Insights from field experiments and numerical modelling

Christopher S. Brown [a,b,*], Isa Kolo [b], Gioia Falcone [b], Daniel Friedrich [c], Sean M. Watson [b,d]

[a] British Geological Survey, Keyworth, Nottingham NG12 5GG, UK
[b] James Watt School of Engineering, University of Glasgow, Glasgow G12 8QQ, UK
[c] School of Engineering, Institute for Energy Systems, University of Edinburgh, Colin Maclaurin Road, Edinburgh EH9 3DW, UK
[d] TownRock Energy, East Woodlands House, Dyce, Aberdeen AB21 0HD, UK

ARTICLE INFO

Keywords:
Thermal performance test
Thermal response test
Cheshire geoenergy observatory
Geothermal
Ground source heat pump
Underground thermal energy storage

ABSTRACT

Decarbonisation of the heating and cooling sectors is essential for achieving net zero targets, and geothermal systems provide a promising pathway to reduce reliance on fossil fuels. To design and optimise ground source heat pump (GSHP) systems, an understanding of subsurface thermal properties is critical. Traditionally, this is achieved through thermal response tests (TRTs), which measure subsurface behaviour under constant heat flux conditions. However, thermal performance tests (TPTs) offer an alternative approach by applying a constant inlet temperature, allowing not only the determination of effective thermal conductivity but also an assessment of the system's thermal capacity under both heating and cooling scenarios. This study presents what is believed to be the UK's first documented TPT and a new direct comparison of heat injection and extraction tests, aiming to demonstrate the method's value for characterising geothermal systems in real-world applications.

The experiments at the Cheshire Geoenergy Observatory consisted of two borehole heat exchangers (BHEs) injecting heat at a constant temperature of 30 °C and two BHEs extracting heat by circulating fluid at a set point of 1 °C within the Sherwood Sandstone Group. Results indicate that TPTs provided effective thermal conductivity estimates (2.43–3.65 W/mK) consistent with core measurements and numerical models. However, there are issues with heat extraction TPTs, which appear to under-estimate thermal conductivity. This could be due to (i) natural convection enhancing heat transfer in the subsurface during heat injection mode, or (ii) the oscillatory behaviours of heaters and chillers may introduce errors when estimating properties, potentially impacting this conclusion.

1. Introduction

It is essential that the heating and cooling sectors are decarbonised to achieve net zero carbon emissions targets by 2050. Geothermal energy can support this with it anticipated that there will be significant growth in the subsurface geothermal sector with specific focus on ground sourced heating and cooling systems. Moreover, the UK government has targeted the installation of 600,000 heat pumps annually by 2028 (HM Government, 2023); however, the current number of ground source heat pumps (GSHPs) installed is ~55,210 (Gonzalez Quiros et al., 2024) with deployment rates of around 4000 installations per year (Abesser et al., 2023). Thus, there is an urgent need to boost installation rates to meet targets and enable decarbonisation.

1.1. Ground source heat pumps

GSHPs operate by exchanging energy with the ground, either extracting or rejecting heat, then transferring this to a building efficiently for heating or cooling. Electrical energy is required to drive a heat pump through a compressor, and such systems often result in 50–70 % energy savings in comparison to traditional technologies (Raymond, 2018). Typically, heat is extracted from the ground through shallow (<2 m deep) collectors, or through vertical borehole heat exchangers (BHEs). BHEs targeting shallow schemes (<500 m deep) often utilise a U-tube configuration due to the ease of installation, whilst deep BHEs use a coaxial configuration, which consists of a pipe inserted within the borehole and fluid is circulated within the annular space, warming with

* Corresponding author at: British Geological Survey, Keyworth, Nottingham NG12 5GG, UK.
E-mail address: cbrow@bgs.ac.uk (C.S. Brown).

https://doi.org/10.1016/j.geothermics.2026.103658
Received 3 July 2025; Received in revised form 20 January 2026; Accepted 2 March 2026
Available online 7 April 2026

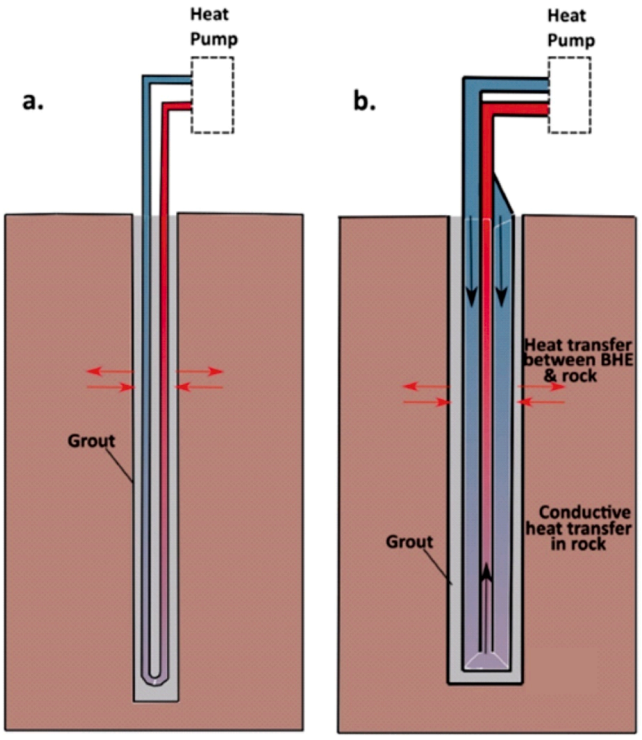

Fig. 1. Comparison between (a) U-tube and (b) coaxial borehole heat exchangers (modified from Brown et al., 2024).

depth, before being circulated to the surface through the central pipe (Fig. 1). Similarly, for U-tube configurations fluid is circulated up and down each shank, exchanging heat or cold energy through the cementitious grout. The coaxial configurations enable greater heat extraction at depth due to maximised surface areas and lower borehole thermal resistance, whilst minimising parasitic losses associated to a circulation pump (Brown et al., 2024).

GSHP systems require careful consideration of system design to ensure sufficient length/depth and spacing of BHEs to ensure there is not thermal interference (e.g., Receveur et al., 2024). This is typically, decided using short-term testing (i.e., thermal response tests – TRTs); however, long-term monitoring can also help to improve operation, define system efficiency and help to maintain sustainable operation of the ground. Chen et al. (2021) analysed the performance of a GSHP system in Leicester, UK, showing that there was a thermal imbalance in the subsurface which creates a shifting of the thermal load in the ground and inefficient operation. Heim et al. (2024) presented data of 40 BHEs to a depth of 100 m's with high spatial and temporal resolution. Cai et al.

Table 1
Parameter table for the experiments.[1] specific heat capacity from Waples and Waples (2004), [2] saturated density derived from the TH0424 final data pack - Contains NERC materials ©NERC 2024, [3] from GEOTHERM-X (2025).

Parameter	Value (hot/cold)	Units
Saturated ground volumetric heat capacity[1,2]	1824,350	J/(K m^3)
Working fluid flow rate (per borehole)	0.5	L/s
Working fluid density (28 % glycol)	1039/1049	kg/m^3
Working fluid specific heat capacity	3805	J/(kg K)
Working fluid thermal conductivity	0.6	W/(m.K)
Dynamic working fluid viscosity	0.0008/0.002	kg/(m s)
Cement thermal conductivity[3]	2	W/(m.K)
Cement density	1650	kg/m^3
Cement specific heat capacity[3]	900	J/(kg K)
Borehole diameter	0.152	m
Depth	100	m
HDPE U-tube Outer Diameter	40	mm
HDPE pipe thickness (SDR11)	3.7	mm
Inlet temperature set point	30/1	°C
Shank spacing (centre to centre)	104.6	mm

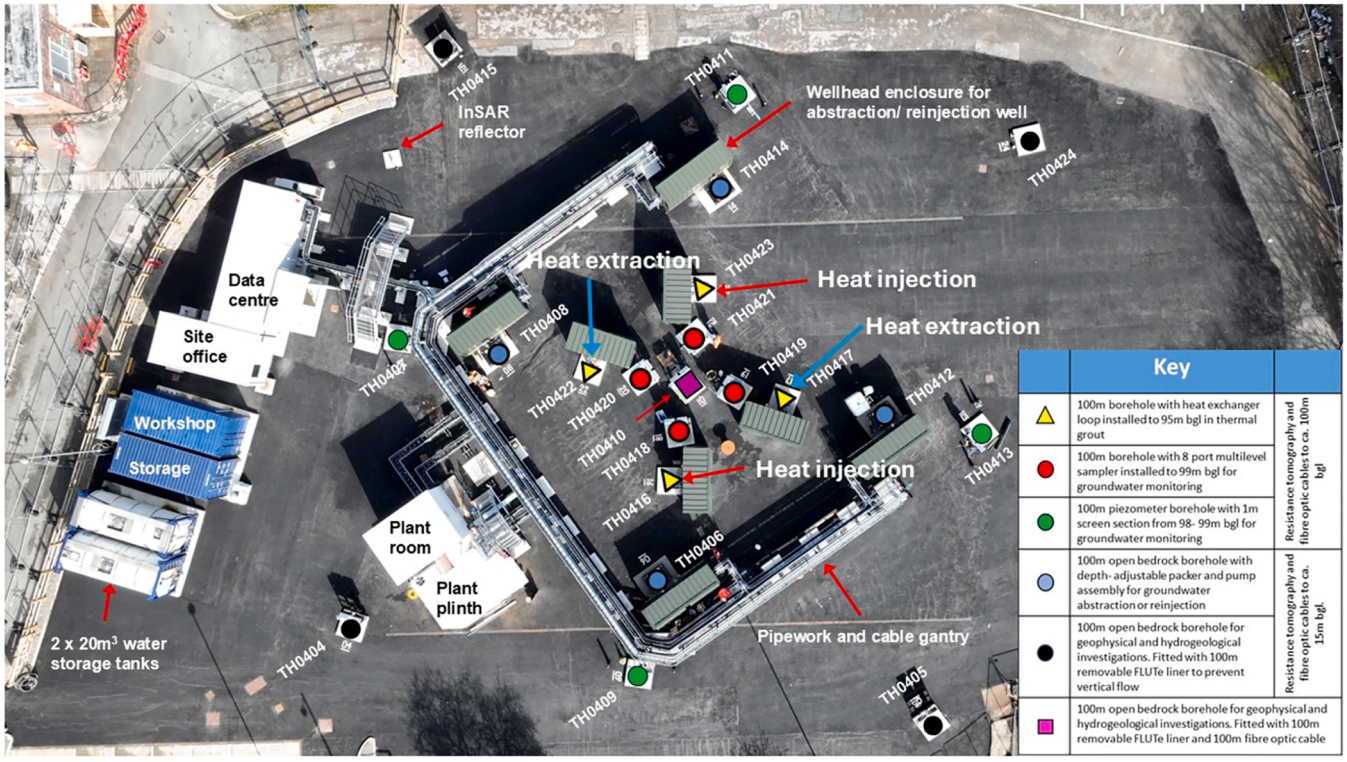

Fig. 2. Aerial photo of the site highlighting borehole locations. Note the yellow triangles are the 4 borehole heat exchangers used in the experimental set up. BGS © UKRI.

Table 2
Borehole grid coordinates and set point temperatures. Taken from BGS GeoIndex Onshore (2025).

Borehole	Grid Coordinates	Set point temperature	Average undisturbed ground temperature
TH0416	344,940.13, 375,841.09	30 °C	12.2509
TH0417	344,947.75, 375,844.81	1 °C*	12.1679
TH0422	344,936.3, 375,848.71	1 °C*	12.1365
TH0423	344,944.03, 375,852.43	30 °C	12.3494

* Note that the inlet temperature entering the cold BHEs was closer to 2 °C and the average undisturbed ground temperature is averaged temperature over the length of the borehole.

(2021) investigated deep BHEs in Xi'an, China, using a pilot system for heat extraction from 5 BHEs to 2 km. They investigated the long-term potential using numerical modelling, following analysis of the monitoring data which was for 106 days in total. Viesi et al. (2018) investigated the potential thermal interference between BHEs during multiple years of operation. Many have considered the long-term monitoring of GSHP over yearly operation which can provide insights into subsurface thermal balancing, surface system performance and the wider longevity of the coupled system. They can provide important information regarding the thermal response of the ground; however, they typically require prior short-term testing, which helps to determine the key ground properties (such as thermal conductivity) to decide on the overall system design and operation.

1.2. Short-term thermal testing

At present, the in-situ subsurface ground properties around closed-loop BHEs are often characterised using TRTs. This involves circulating a fluid around the BHE with a known heating or cooling load, allowing the subsequent calculation of the effective thermal conductivity of the ground and borehole thermal resistance by monitoring the exchange of hot and cold thermal energy through the borehole wall (e.g., Gehlin, 2002). The heat load, predetermined by a heater or chiller, is usually constant, although stepped tests are often used and the heat load relates to the flow rate, difference in temperature between the inlet and outlet fluid, and volumetric heat capacity of the fluid. The average fluid temperature is then determined and analysed using analytical or numerical models. Typically, the infinite line source (ILS) (i.e., Signorelli et al., 2007; Wagner et al., 2012; Choi and Ooka, 2015; Angelotti et al., 2018) or infinite cylindrical source (ICS) (i.e., Priarone et al., 2015; Yu et al., 2016; Zarrella et al., 2017) methods are adopted, using regression analysis or parameter-estimation techniques (e.g., Li et al., 2024).

TRTs are becoming a common tool internationally to determine in-situ properties to improve the operation and design of GSHP systems.

Fig. 3. Pictures of the equipment used during testing: (a) chiller for the heat extraction mode borehole heat exchangers, (b) control valves between the surface piping and borehole heat exchangers, (c) control valves between the chiller/heater and outer pipework, and (d) connection to the wellhead for the inlet and outlet fluid.

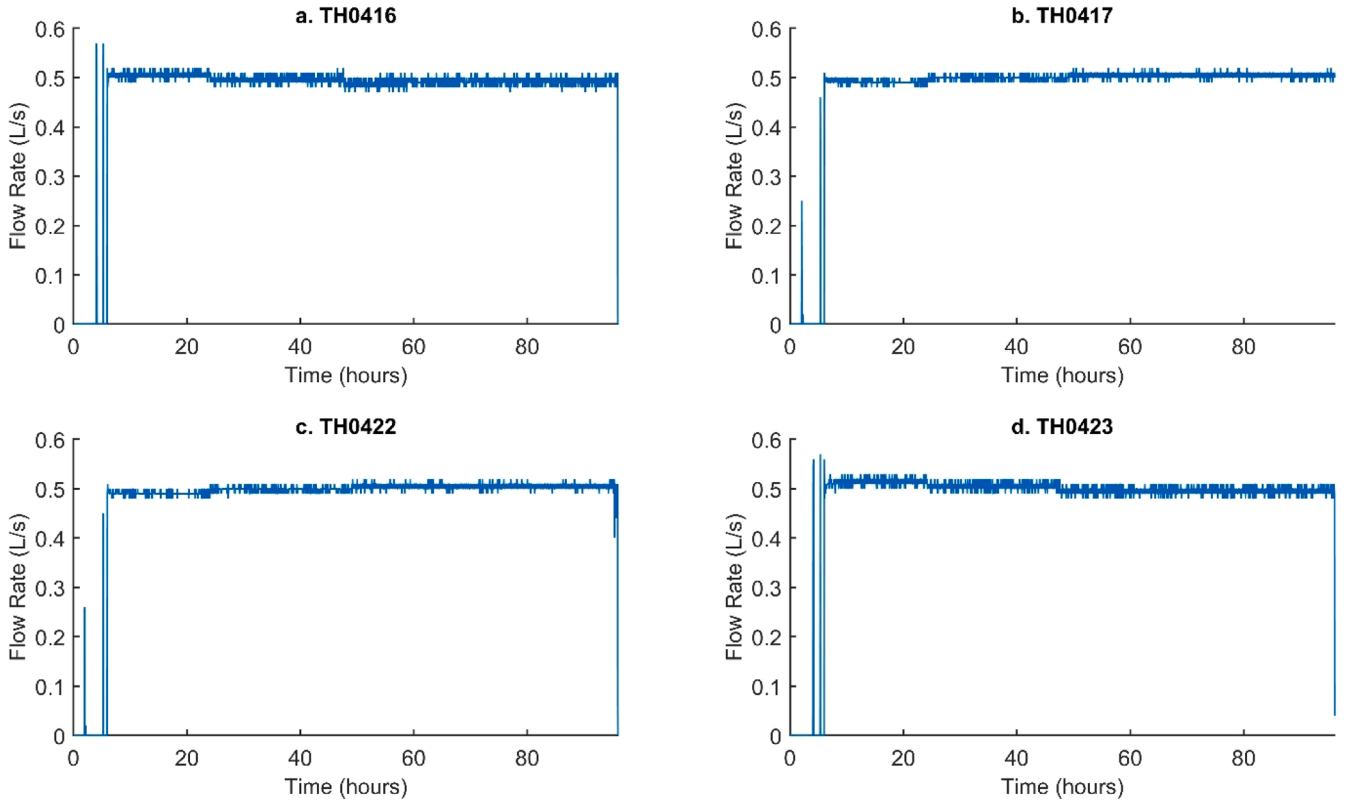

Fig. 4. Flow rates held constant for the duration of the experiment at 0.5 L/s for BHEs (a) TH0416, (b) TH0417, (c) TH0422, and (d) TH0423.

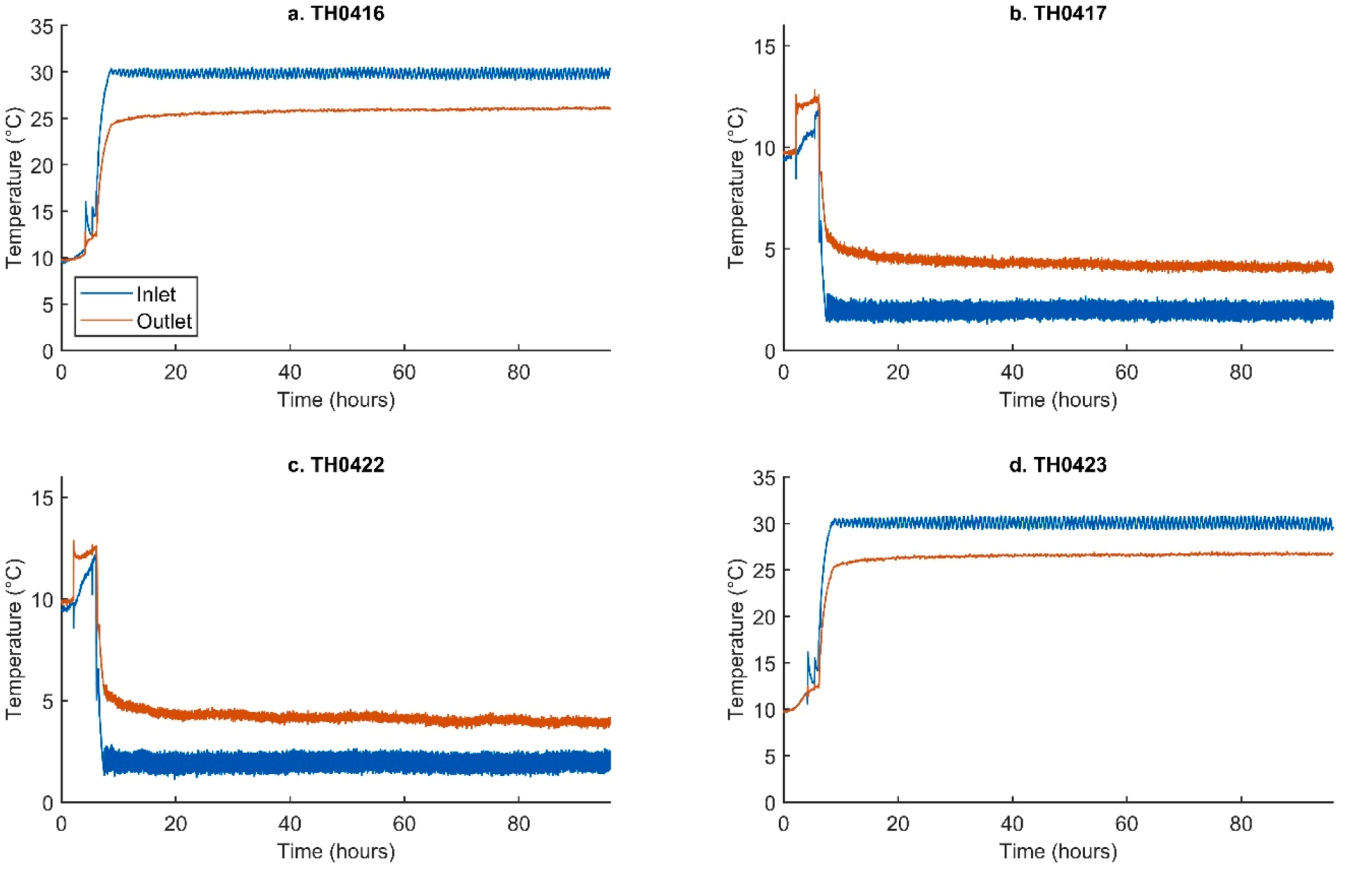

Fig. 5. Inlet and outlet temperatures for the duration of the experiment for BHEs (a) TH0416, (b) TH0417, (c) TH0422, and (d) TH0423. Note set points of 30 °C and 1 °C for heat injection and extraction boreholes, respectively.

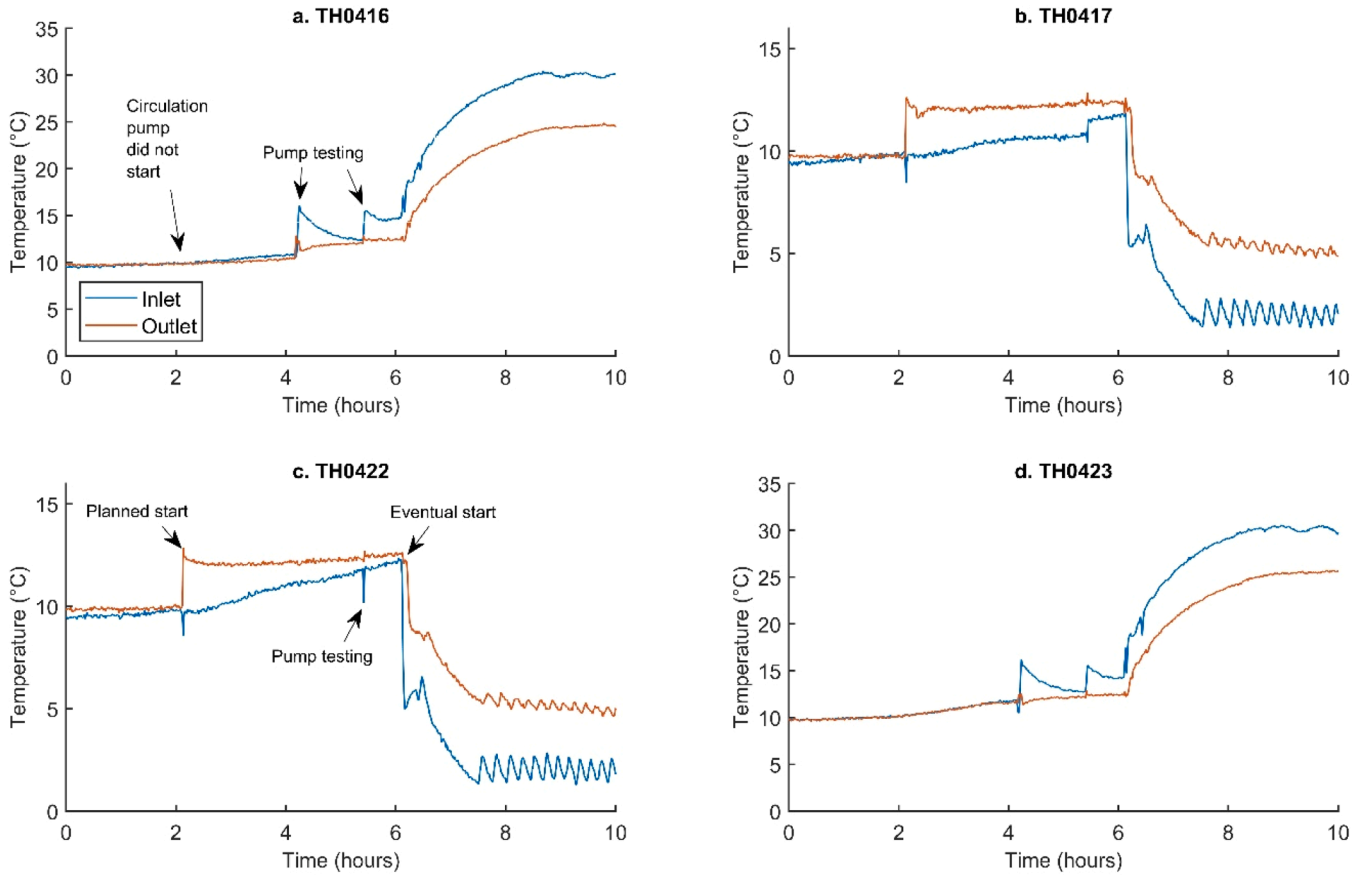

Fig. 6. Inlet and outlet temperatures for the first 10 h of the experiment for BHEs a) TH0416, b) TH0417, c) TH0422, and d) TH0423. Note set points of 30 °C and 1 °C for heat injection and extraction boreholes, respectively.

Analysis has been undertaken in a wide range of countries including the UK (Banks et al., 2013), China (Zhang et al., 2018), Sweden (Eklöf and Gehlin, 1996), and Turkey (Esen and Inalli, 2009), among others. Parametric variation has been widely investigated on the impact on TRTs through numerical and experimental investigation. It has been shown that poor grouting is detrimental to borehole performance during a TRT, double U-tubes provide better performance compared to single U-tubes (due to lower thermal resistance) and low flow rates within the laminar range are associated with high borehole thermal resistance (Banks *et al.*, 2009). Others have highlighted that shank spacing (the distance between inlet and outlet pipes), a higher initial geothermal gradient, thermal dispersion and convection can also impact TRTs (Wagner et al., 2012).

Models have been developed allowing the rapid analysis of TRT datasets (e.g., Beier, 2024; Wang et al., 2025), with the analytical model from Beier (2020) also forming an additional tool for long-term deep coaxial constant base load analysis adopted by several works, showing minimal discrepancy in comparison with numerical models (e.g., Cai et al., 2022; Brown et al., 2023a; Banks et al., 2024; Charlton and Rouainia, 2025). Different analytical and numerical methods for interpreting TRTs can however, lead to different interpretation of ground properties. Oh et al. (2025) highlighted in their case study that thermally enhanced grouts could result in an underestimation of the ground properties using the ILS method in contrast to the ICS method. Brown et al. (2023b) highlighted that different numerical and analytical solutions produce different estimates of inputted thermal properties through forward modelling. Beier (2021) showed that a range of analyses have relatively similar discrepancy when analysing constant inlet temperature TRTs. Furthermore, several reviews have been undertaken highlighting varying types of TRTs, case study evaluations and critical literature appraisals (e.g., Rainieri et al., 2011; Raymond et al., 2011; Zhang et al., 2014; Spitler and Gehlin, 2015; Wilke et al., 2020).

New innovative types of 'advanced' TRTs have also been developed. These have focused on distributed TRTs (e.g., McDaniel et al., 2018; Hart et al., 2022; Attri et al., 2023; Seib et al., 2025), cables that are heated within the U-tube with no fluid flowing (Raymond et al., 2010, 2015), flow-rate controlled TRTs (Aydin et al., 2024) and controlled inlet temperature TRTs (Aydin et al., 2017; Aydin et al., 2019; Choi et al., 2019). Distributed TRTs are used to observe different subsurface heat transfer along the borehole providing vertical changes in thermal conductivity related to different heat injection rates, heated cables often are more cost effective as they require lower power sources and can provide distributed thermal conductivity values, and flow-rate controlled TRTs change the flow rate to maintain a near constant inlet and outlet fluid temperature. Constant inlet temperature TRTs, also known as a thermal performance test (TPT), have low reporting in literature but seems to be more commonly used for energy pile testing than conventional GSHPs (Choi et al., 2019). TPTs involve novel analysis of the subsurface using a constant inlet temperature fluid being circulated, in contrast to a temperature difference imposed by the capacity of a heater used in TRTs. Aydin et al. (2019) were able to predict thermal conductivity values for the ground from field data and numerical modelling with limited discrepancy to true values when using TPTs. Similarly, Choi et al. (2019) also conducted numerical and experimental testing, highlighting the fact that TPTs can allow determination of thermal properties far quicker than traditional TRTs. Jia et al. (2019) also undertook simultaneous experiments to determine ground properties with TPTs using heat injection and extraction tests. The accuracy of TPTs have also been compared by others who have proven them to be similar to TRTs (e.g., Beier, 2021).

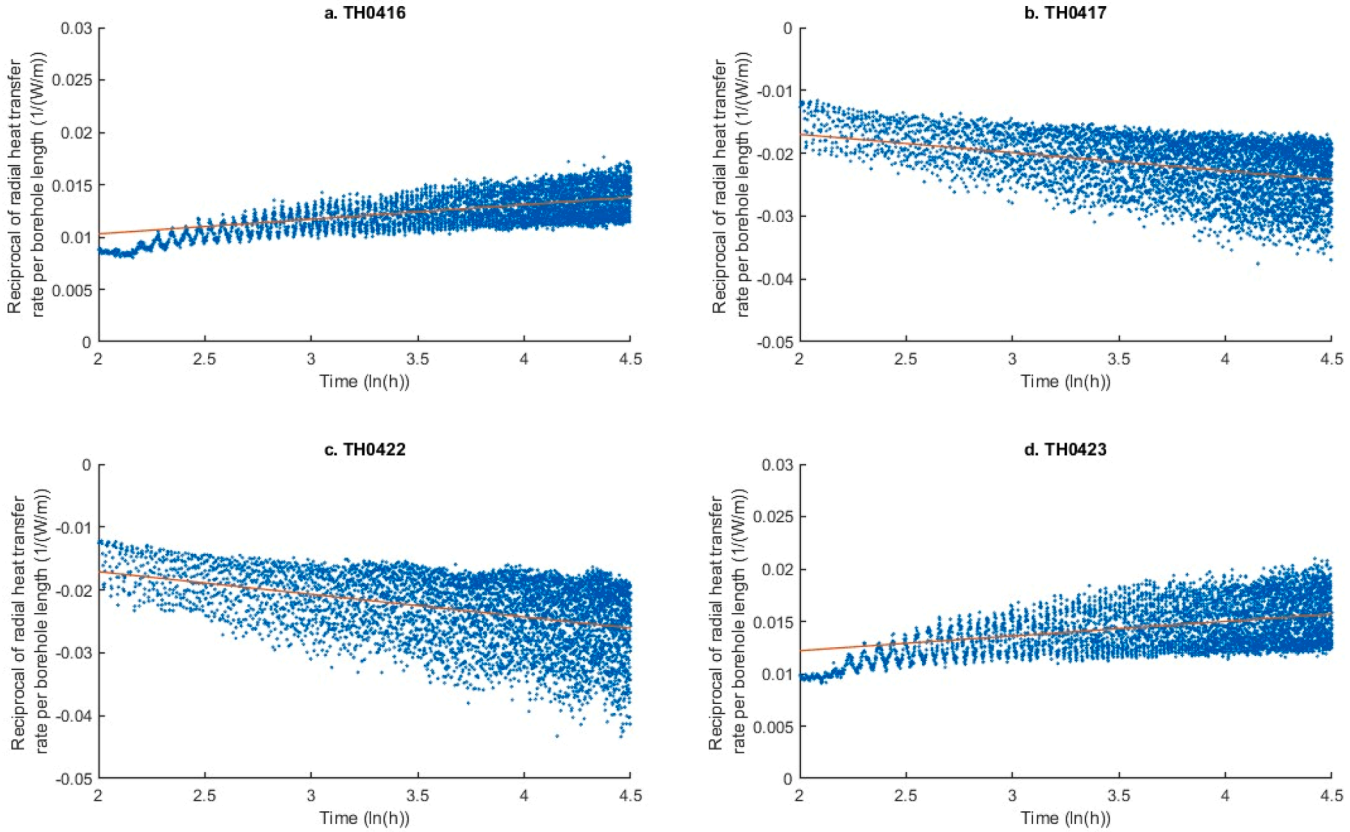

Fig. 7. Semi-log plots for 24–94 h for the reciprocal of the radial heat transfer rate per borehole length against time for BHEs (a) TH0416, (b) TH0417, (c) TH0422, and (d) TH0423. Note the negative values indicate the heat extraction boreholes and the trendline is highlighted in orange.

Table 3
Estimated bulk thermal conductivity over the lengths of the boreholes.

Borehole	Estimated Thermal Conductivity (W/mK)
TH0416 (Heat injection)	3.65
TH0417 (Heat extraction)	3.03
TH0422 (Heat extraction)	2.43
TH0423 (Heat injection)	3.56

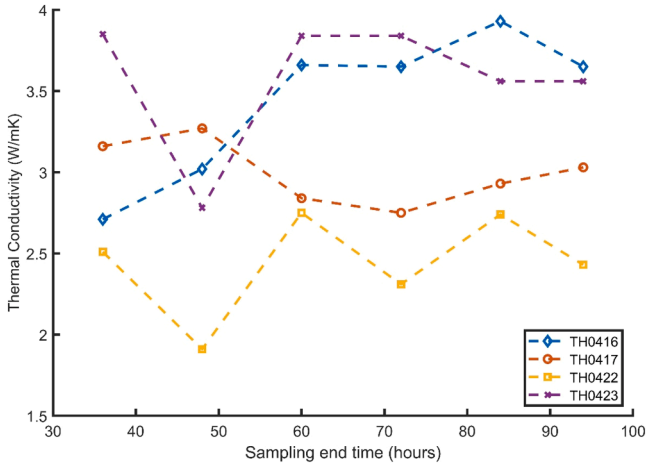

Fig. 8. Estimated effective thermal conductivity for a range of sampling windows. Time was sampled from 24 h to the time plot shown on the graph.

1.3. Objectives of the study

Present literature is typically focused on TPTs that use heat injection via a constant inlet temperature, with few TPTs documented extracting heat by setting an inlet temperature lower than the subsurface temperature using a chiller. Thus, the paper evaluates a new set of field test data that compares heat injection and extraction TPTs to measured in-situ thermal conductivity data from cores and data from forward-modelling using numerical models. The UK Geoenergy Observatory in Cheshire was chosen to facilitate TPTs as it has world class facilities, with high data recording capabilities (e.g., Bowes et al., 2023). It is based in the Cheshire Basin, which has high-quality aquifers of Permo-Triassic age and a significant geothermal potential (e.g., Downing and Gray, 1986; Rollin et al., 1995; Jackson, 2012; Brown, 2023). Four BHEs were analysed which utilise U-tube configurations, installed to 100 m depths, with further facility details described in the methods section. It is believed this study provides one of the first documented TPTs in the UK, and a novel comparison between heat injection and extraction TPTs.

2. Methods

2.1. Experimental set-up

The experiment was undertaken at the Cheshire UK Geoenergy Observatory, where a world class facility has been established in recent years consisting of high-quality sensing capabilities for open- and closed- loop testing. 21 vertical boreholes were drilled to 100 m, with 4 of these consisting of 40 mm outer diameter (OD) high density polyethylene U-tube BHEs (highlighted as TH0416, TH0417, TH0422, TH0423 in Fig. 2). The boreholes penetrate the Chester Formation of the

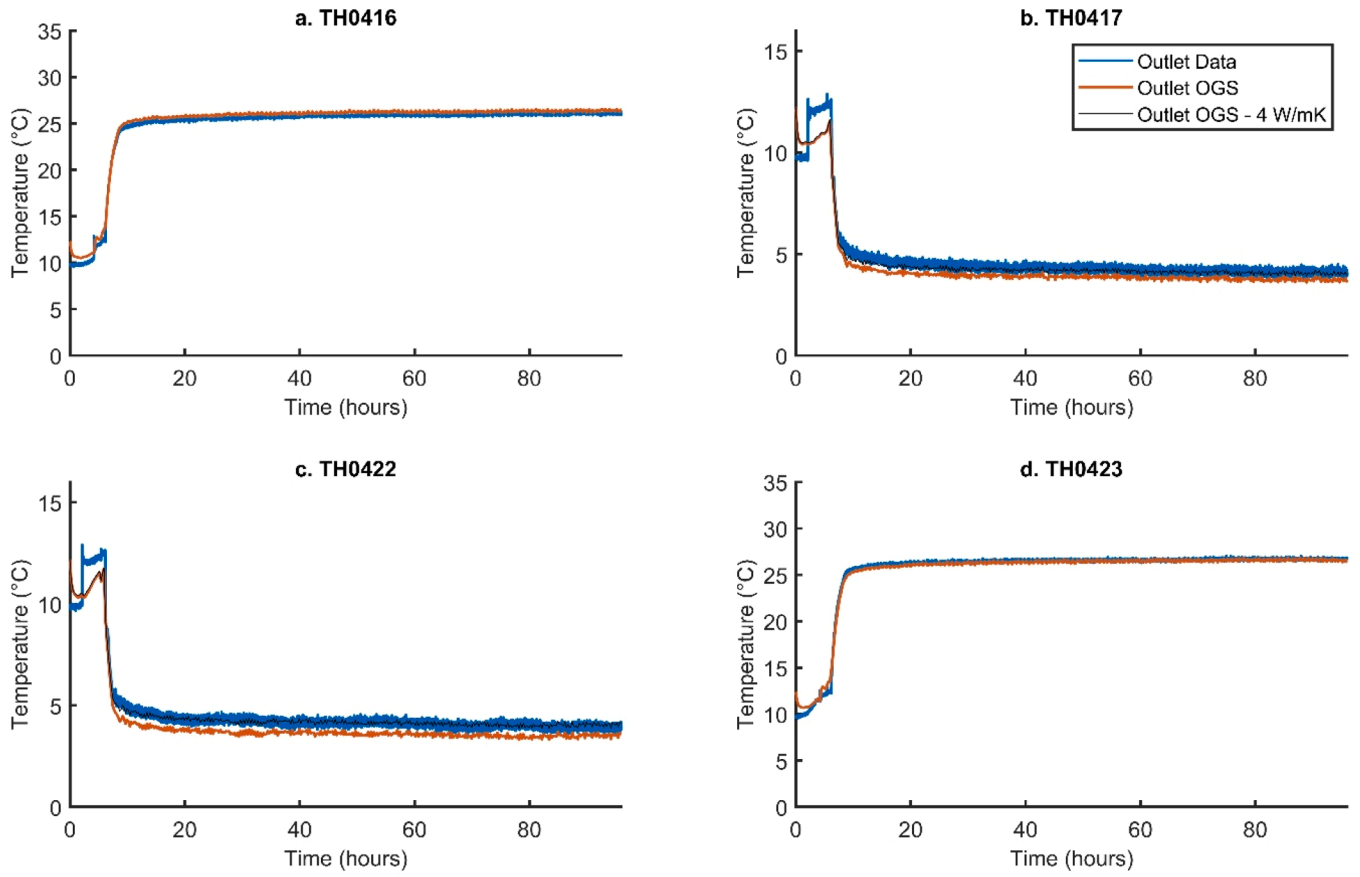

Fig. 9. Outlet temperatures for the duration of the experiment for BHEs (a) TH0416, (b) TH0417, (c) TH0422, and (d) TH0423. Note the inlet for the numerical model was set identical to that for each borehole recorded in the raw data.

Sherwood Sandstone Group, with bedrock exposed from surface, albeit now covered by a thin layer of man-made material (<2 m thickness) (Bowes et al., 2023). Further parameters are listed in Table 1, with grid coordinate and specific fluid/undisturbed temperatures in Table 2.

The experiment used a 16 kW chiller and 24 kW heater (Fig. 3) connected to separate flow circuits feeding heated and cooled BHEs simultaneously. Two BHEs were cooled using an inlet temperature with a set point of 1 °C for the heat extraction experiment (TH0417 and TH0422), and two BHEs were heated with a set point of 30 °C for the heat injection experiment (TH0416 and TH0423). For the cold, heat extraction circuit the chiller regulates the cold buffer tank temperature and not the wellhead temperature. Thus, it should be noted that the inlet temperature recorded at the top of the wellhead for the cold side was closer to 2 °C which is anticipated to be due to heat gain from piping in the surface infrastructure, or the circulation pump. For the experiments, heat was injected into boreholes TH0416 and TH0423, whilst heat was extracted from boreholes TH0417 and TH0422 (Table 2). The flow rates were controlled at 0.5 L/s for the duration of the experiments (Fig. 4).

The experiments began on the 24th February 2025, with an anticipated start time of 11am (hour 2 on Figs. 5 and 6); however, both circulation pumps failed to operate on the heat injection side due to a loose connection in the building management system (BMS) panel. This led to some small-scale heat injection/extraction events appearing to occur prior to operation which were to test the system (Figs. 5 and 6). Following a prompt equipment fix, the tests recommenced at 15:00, with both sets of inlet temperatures for heat injection and heat extraction TPTs reaching close to the set points within 2.5 h. The tests were then monitored and stopped on 28th February at 09:00. This resulted in the TPTs lasting for 90 h (note they formally start at 6 h in Figs. 4, 5 and 6). At the start of the experiment, the circulation fluid was measured to contain 28 % glycol. The fluid inlet and outlet temperatures were measured at ground level for all heat exchangers.

2.2. Governing equations

2.2.1. Thermal response test

The fluid temperature in a TRT is often calculated using Kelvins line source theory (e.g., Carslaw and Jaeger, 1959), which is known as the infinite line-source approach. It assumes the ground is an unbound media, with an initial steady state temperature, homogenous properties and heat transfer only occurring in the radial direction, whilst neglecting end effects and axial heat transfer (e.g., Brown et al., 2023b; Maghrabie et al., 2023):

$$\overline{T}_{wf} - T_{\infty} \approx q.R_b + \frac{q}{4\pi\lambda}\left[\ln\left(\frac{4\alpha t}{(r_e)^2}\right) - \gamma\right] \quad (1)$$

where α is the thermal diffusivity, γ is Euler's constant, q is the heat injection rate per meter of the borehole length, r_e is the equivalent radius, λ is the effective thermal conductivity, $\overline{T}_{wf}$ is the averaged fluid temperature ($\overline{T}_{wf} = \frac{(T_{in}+T_{out})}{2}$), T_{∞} is the averaged undisturbed ground temperature, T_{in} is the inlet temperature to the BHE and T_{out} is the outlet temperature from the BHE. As heat transfer in the ground is simplified to a one-dimensional problem, using conduction only, the average fluid temperature of the circulating fluid in the borehole can be written in a linear form (e.g., Zhang et al., 2014):

$$\overline{T}_{wf} = k\ln(t) + m \quad (2)$$

As the gradient (k) is proportional to the heat rate and thermal conductivity ($k = \frac{q}{4\pi\lambda}$), the effective thermal conductivity can be

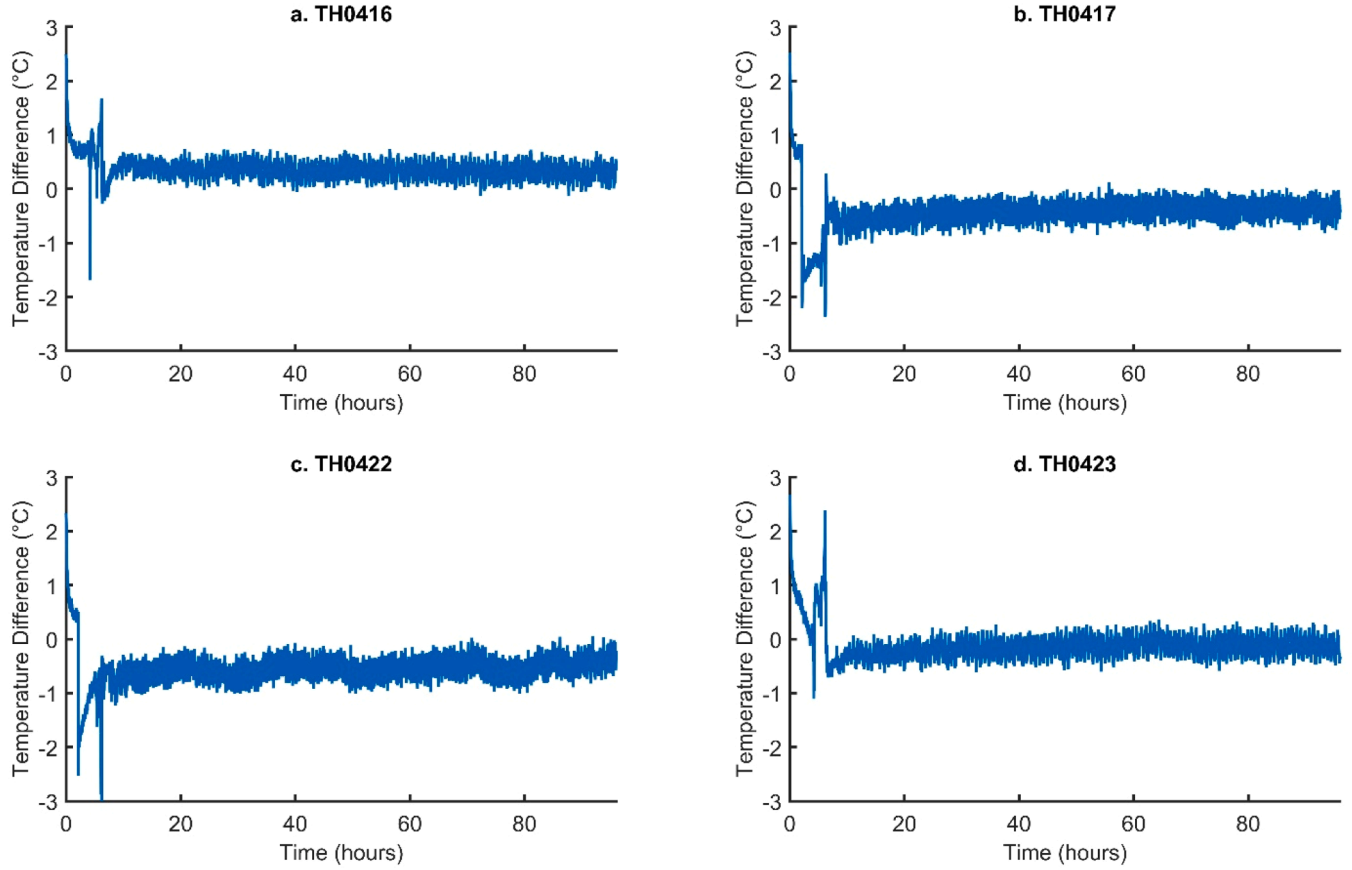

Fig. 10. Difference in outlet temperatures between the numerical model and raw data for the duration of the experiment for BHEs (a) TH0416, (b) TH0417, (c) TH0422, and (d) TH0423.

determined using the gradient of the line when plotting the average fluid temperature against the natural log of time ($\ln(t)$). Note m is the intercept on the y-axis. Line source theory is valid beyond a certain critical time (e.g., Ingersoll et al., 1954; Gehlin, 2002) and TRTs are often performed over a period of 30–60 h but there is no prescribed guideline for test duration (Raymond et al., 2011), although the borehole should reach steady-state conditions for validity of the method (Wilke et al., 2020).

2.2.2. Thermal performance test

It has been highlighted in literature that the effective thermal conductivity of the ground can also be determined using TPTs with controlled inlet temperature. Aydin et al. (2019) developed a novel solution where the reciprocal of radial heat transfer per depth of a borehole ($\frac{1}{q'(t)}$) is given as:

$$\frac{1}{q'(t)} = \beta\left[\ln(t) + \ln\left(\frac{4\alpha}{e^{\gamma}(r_e)^2}\right)\right] \tag{3}$$

where $\beta = \left[\frac{1}{4\pi\lambda\left(\overline{T}_{wf} - T_{\infty}\right)}\right]$ is the slope of the logarithmic time scale in Eq. 3., and t is time. The effective thermal conductivity (λ) can thus be calculated using regression analysis of the gradient (i.e., β) and estimated as:

$$\lambda = \frac{1}{4\pi\beta\Delta T} \tag{4}$$

where $\Delta T = \overline{T}_{wf} - T_{\infty}$. This is calculated from 24 h to the end of the simulation as the heat exchange fluid is still warming up to the set point and to minimise any borehole effects as the BHE is reaching thermal equilibrium. TPTs have the benefit of not requiring an estimated volumetric heat capacity in contrast to TRTs, and they can provide an estimate of the specific heat injected/extracted into the ground which can allow the determination of the thermal power of the system.

2.3. Numerical model

Numerical modelling was also undertaken to forward model the TPTs and evaluate the suitability of derived effective thermal conductivities. The numerical model was developed using the BHE module of the multi-physics finite element code, OpenGeoSys (OGS) (Kolditz et al., 2012). It uses a dual-continuum model in which the BHE is discretised using one-dimensional finite elements while the surrounding rock medium is discretised with three-dimensional finite elements. A simplified set-up is assumed for the BHE with the U-tube BHE inserted within a grout area that separates it from the surrounding rock (see Fig. 1). While heat transfer is assumed to be conduction for the grout and surrounding rock, convection is also considered for the flow in the BHE. Energy balance is solved for the surrounding rock, the grout region and the BHE. For details on the governing equations and accompanying boundary conditions for the interaction between BHE components and surrounding rock, those interested can refer to Shao et al. (2016); Chen et al. (2019); Kolo et al. (2023). Results from OGS have been extensively validated against experimental data (e.g. Brown et al., 2024; Cai et al., 2021) (although not against TPTs until this study), and verified against other numerical/analytical results (Brown et al., 2023c; Kolo et al., 2025), providing high levels of confidence in the software.

A rock domain of 400 m × 400 m × 200 m (x, y, z) was used with the 100 m BHE centralised in the domain. This leaves 200 m between the BHE and the lateral boundary, and 100 m from the basal boundary to the BHE, thereby avoiding any thermal interactions with the boundary.

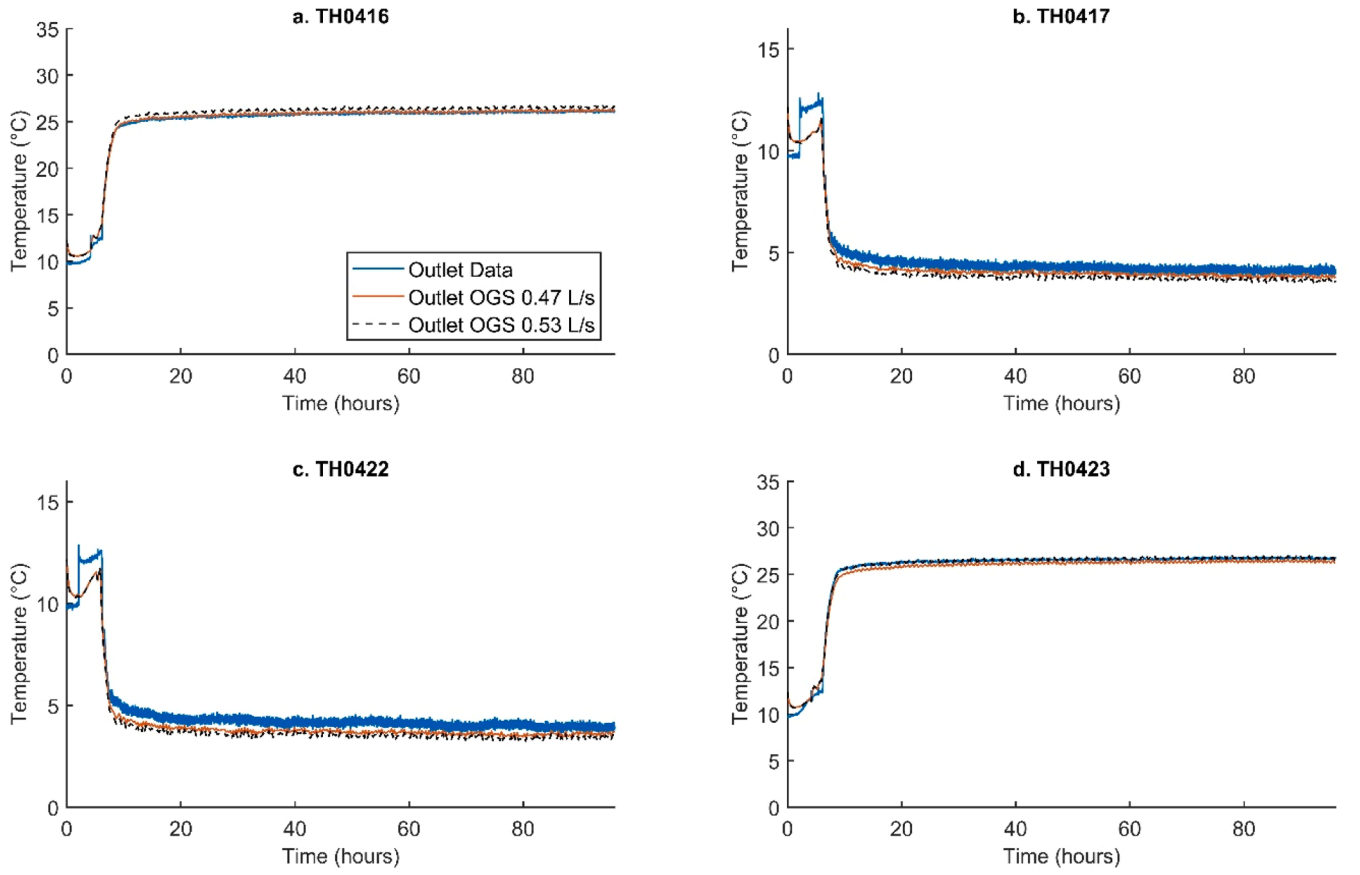

Fig. 11. Outlet temperatures for the modelled and experimental data for varied flow rates for BHEs (a) TH0416, (b) TH0417, (c) TH0422, and (d) TH0423. Note the inlet for the numerical model was set identical to that for each borehole recorded in the raw data.

Neumann no-flow boundaries were applied to the sides and base of the model, whilst the top was fixed Dirichlet using the same temperature as the average rock domain for each simulation. Since there was no thermal interaction among the BHEs during the test due to the large borehole spacing (~8.5 m), only one BHE was modelled independently at a time to determine the respective effective thermal conductivities around each borehole. This was confirmed by checking if there was any change in temperatures in the central boreholes in comparison to conditions before the experiment started (TH0410, TH0418, TH0419, TH0420, TH0421- see Fig. 2 for locations). Under initial conditions the temperature profile was set up with the average undisturbed ground temperature used as a constant (see Table 2) and it was assumed that all BHE components were in thermal equilibrium with the ground. The inlet temperature at the top of the BHE was prescribed as identical to that from the tests, a constant flow rate of 0.5 L/s was used and, a minimum and maximum time step of 1 s and 15 min was used, respectively. All parameters were modelled as of Tables 1 and 2.

3. Results

3.1. Thermal performance test

As already stated, during the test, heat was injected into boreholes TH0416 and TH0423, whilst heat was extracted from TH0417 and TH0422. This is highlighted in Figs. 5 and 6, which show the full duration of the experiment and a zoomed in section on the first 10 h, respectively. For the heat injection boreholes, the set point (30 °C) was achieved within the first 2 and a half hours, whilst for the heat extraction boreholes (close to) the set point (1 °C) was achieved within 2 h. Fluid temperatures were recorded at the wellhead every minute, taken as an average over a 7 s interval. There are also noticeably large oscillations in both the inlet and outlet fluid temperature associated to cycling of the chiller and heater when attempting to meet the set point. A variation in amplitude of the wellhead measured temperature occurred up to ~0.8 °C either side of the average injection temperatures (30 °C and 1 °C for hot and cold tests, respectively). It was also observed that in the heat injection boreholes (TH0416 and TH0423) the outlet temperature is lower than the inlet fluid temperature as the ground is gaining heat, warming with time. Whilst in contrast, the outlet fluid temperature is higher in the heat extraction as the ground is losing heat.

Fig. 7 shows the application of the Aydin et al. (2019) method of determining the effective thermal conductivity by plotting the reciprocal of the radial heat transfer rate of the borehole on a semi-log plot against time. The data is fitted using the least squares regression method, with the data and fitted data highlighted in Fig. 7. From this, the effective thermal conductivity was estimated using Eq. (4) for each borehole (Table 3). It was observed that the heat extraction TPTs in boreholes TH0417 and TH0422 provide lower thermal conductivity estimates than from the heat injection boreholes. This could be a result of the method of test (i.e., extracting heat, rather than injecting heat which is commonly applied for TRTs), which may create different rates of heat injection/extraction (see Section 3.4), enhanced heat transfer created by local convection during heat extraction (e.g., Witte, 2001; Jia et al., 2019) or due to the noise of the data, which is higher within the heat extraction mode. This level of oscillation in the apparent noise could create issues in determining the effective thermal conductivity values and is assessed further through forward numerical modelling in Section 3.3. Past TPTs have shown some similar oscillatory behaviour around the set point of the inlet temperature typically within 0.2 °C (Jia et al., 2019), whilst other testing methods appear to show greater fluctuations up to a few degrees (Aydin et al., 2024). Similarly, TRTS can also show variability in the input heat rate (e.g., McDaniels et al., 2018).

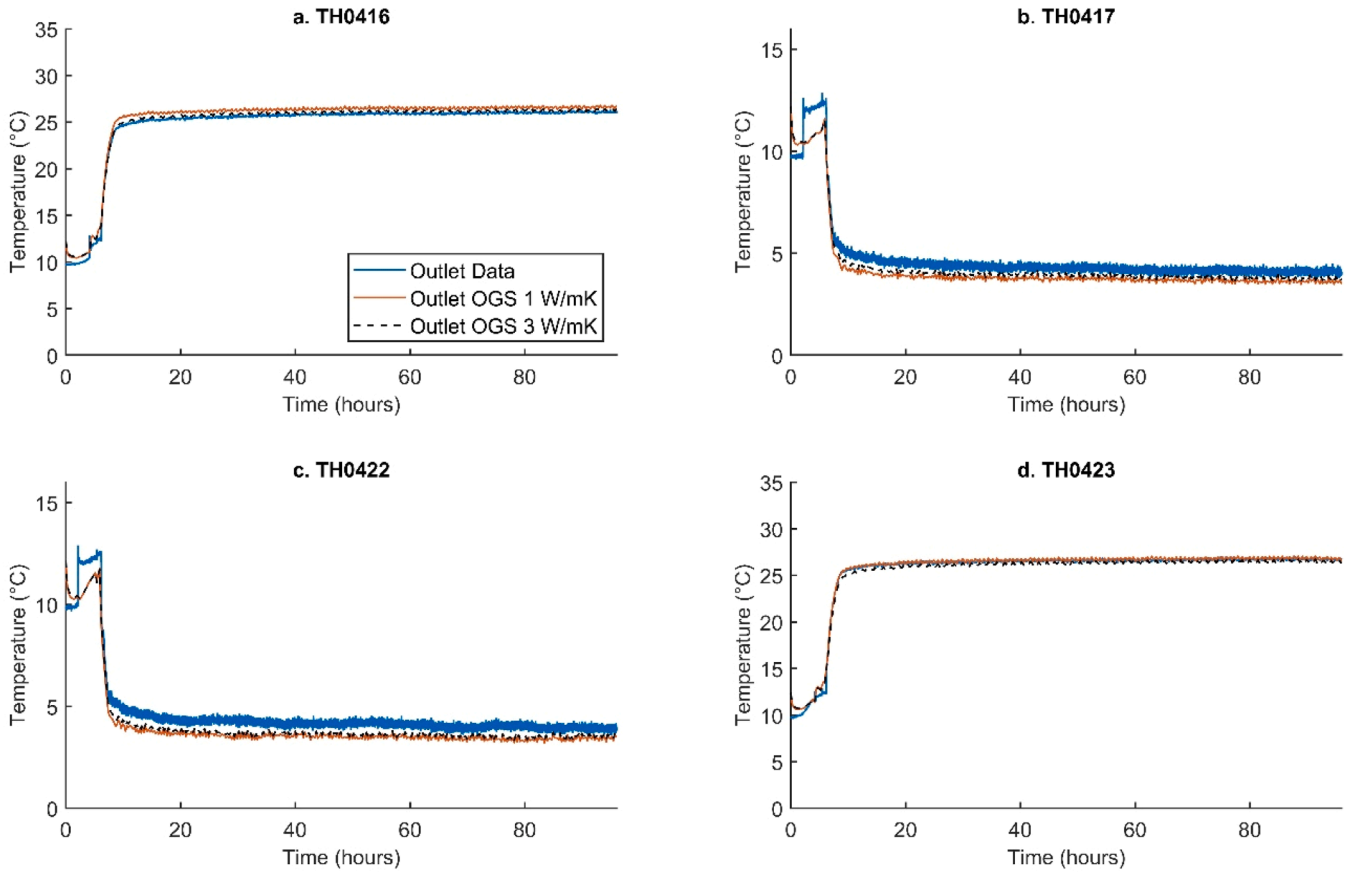

Fig. 12. Outlet temperatures for the modelled and experimental data for varied grout thermal conductivities for BHEs (a) TH0416, (b) TH0417, (c) TH0422, and (d) TH0423. Note the inlet for the numerical model was set identical to that for each borehole recorded in the raw data.

Thus, it is difficult to assess the impact of noise without further analysis in the forthcoming sections.

There were slight variations in the flow rate, this was recorded between 0.47 and 0.53 L/s for boreholes TH0416 and TH0423, with a slight decrease with time. Whilst for boreholes TH0417 and TH0422 there was a slight increase of the flow rate with it ranging between 0.48 and 0.52 L/s. This is interpreted to occur due to the change in density of the fluid as it is heated or cooled with time. This is evidenced when approximating density levels from the glycol density data sheet.

3.2. *Impact of varying temporal sampling resolution*

The sampling time-period used in Eq. (4) was varied to investigate how this may impact the effective thermal conductivity estimates as some have claimed that TPTs can be used at shorter sampling times in contrast to TRTs (e.g., Choi et al., 2019). Fig. 8 highlights the changes in the estimated effective thermal conductivity under varying time samples. The sampling period was extended from 24 h (i.e., on Fig. 8 at time 36 h the time was sampled between 24 h and 36 h). It is evident that there is more variability in the earlier time data. This highlights longer time estimates may provide more accurate estimates of ground thermal conductivity values, whilst it also shows that the noise created by cycling of the heater and chiller may impact these estimates. Thus, when conducting TPTs it is better to use a larger sampling data set which extends for increased time periods focusing on later data in time allowing the nearby heat flow field to reach steady-state. This is in agreement with findings from Aydin et al. (2019) who suggest longer duration TPTs will result in more accurate estimated ground thermal conductivity estimates. However, it is in contradiction to Choi et al. (2019) who suggested that the effects of heat storage reduce quicker than in TRTs and should allow TPTs to be more accurate in shorter experimental duration. In this study, there appears to be no benefit to a shorter TPT.

3.3. *Comparison to numerical simulations*

To further investigate the accuracy of the TPTs and their potential to under- or over-estimate effective thermal conductivity values, simulations were performed using OGS software. The models were set up as per the conditions of the site, with the circulation rate of 0.5 L/s prescribed and the recorded inlet temperature for each borehole was used as the boundary condition for the temperature of the fluid entering the borehole (Tables 1 and 2). For each borehole, the effective thermal conductivity value calculated in Section 3.1 was used (Table 3).

The outlet fluid temperatures for each simulation are displayed in Fig. 9, and the difference in temperature between the data generated on OGS through forward modelling and the data recorded from the experimental set up is shown in Fig. 10. For the heat injection boreholes (TH0416 and TH0423), the generated outlet temperature is extremely close to the experimental, with minimal discrepancy – with <0.5 °C for the whole simulation after the first 12 h when there is more discrepancy associated to the false start of the TPT and subsequent system checks (i.e., Fig. 6). In contrast, for the heat extraction boreholes (TH0417 and TH0422), there is more discrepancy with the modelled data within 1 °C of the experiment (after the first 12 h). By the end of the simulation, both heat extraction boreholes have errors <0.5 °C. Another simulation was also undertaken for each of the heat extraction boreholes with a thermal conductivity value of 4 W/mK as the input value. It was observed that this provided a better fit in comparison to the real data and suggests that the calculated effective thermal conductivity values from the TPT are underestimating the true thermal conductivity; although it should be acknowledged that the effective thermal conductivity also accounts for

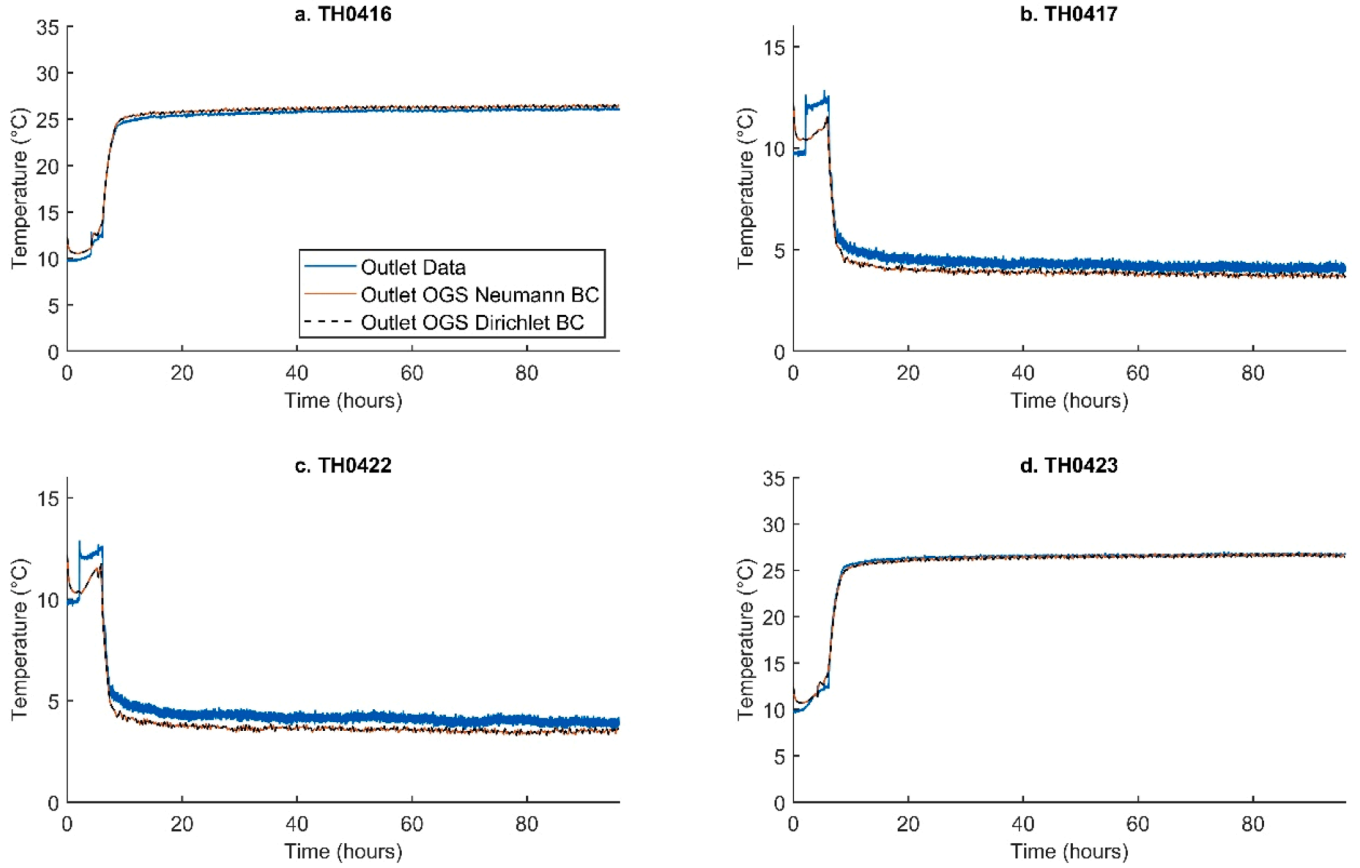

Fig. 13. Outlet temperatures for the modelled and experimental data for varied top surface boundary conditions for BHEs (a) TH0416, (b) TH0417, (c) TH0422, and (d) TH0423. Note the inlet for the numerical model was set identical to that for each borehole recorded in the raw data.

the cementitious grout's lower thermal conductivity which could create this apparent higher thermal conductivity of the ground in the numerical modelling.

Further simulations were carried out to assess whether variations in model parameters and assumptions influenced the forward-modelled TPT results on OGS. First, the fluid flow rate was adjusted to reflect the minimum and maximum observed values (0.47 and 0.53 L/s). Higher flow rates produced only a slight increase in outlet temperature for the heat injection tests, whilst for the heat extraction tests lower flow rates provided higher outlet temperatures closer to the observed outlet data from the experiment (Fig. 11). This correlated to a difference throughout of up to 0.35 °C for the heat injection mode and 0.2 °C for the heat extraction mode between the minimum and maximum flow rates used. It is therefore possible that the flow rate variations (see Fig. 4) have impacted the numerical model results where a constant flow rate was used.

Grout thermal conductivity and model domain boundary conditions were also varied. Grout thermal conductivity was varied between 1 W/mK and 3 W/mK, and Neumann no-flow boundary conditions were also implemented at the surface level instead of the Dirichlet conditions applied. The varied grout resulted in a change of up to 0.4 °C for the heat injection test, and 0.15 °C for the heat extraction test (Fig. 12). Finally, the effect of boundary conditions (i.e., Neumann top surface) had a negligible effect on the modelled outlet temperature (Fig. 13).

A final set of tests examined the influence of noise on the ability of TPT to generate reliable datasets for estimating subsurface in-situ effective thermal conductivity. This was done by modelling a heat injection experiment on TH0416 and heat extraction on TH0417 with constant inlet temperatures of 30 °C and 2 °C, respectively (Fig. 14). The results demonstrated that the models reproduced thermal conductivity values within 15 % of the input parameters when analysed using the method of Aydin et al. (2019), indicating that TPT can provide robust estimates with low noise levels from the input data.

3.4. Thermal power of borehole heat exchangers

The likely thermal power for each scenario can be determined to provide the likely operational capacity in each scenario for heat injection and extraction (Fig. 15). Assuming an injection temperature of heat at 30 °C into the ground and flow rate of 0.5 L/s then the thermal load that could go into the ground would be around 7 kW. This could occur when heat is rejected from cooling loads, or for ambient borehole thermal energy storage. In contrast, without the ground temperature being raised due to thermal energy storage, the maximum load that could be used for extraction would be in the region of 4 kW. For the heat extraction scenario this corresponds to specific heat rates recorded of ~40 W/m and ~38 W/m for boreholes TH0417 and TH0422, respectively. This could thus be used in further calculations for the system longevity when extracting heat. Similarly, for the heat injection boreholes specific heat rates of ~73 W/m and ~69 W/m were calculated for boreholes TH0416 and TH0423, respectively.

4. Discussion

4.1. Sensitivity of temperature measurement equipment

BHE inlet and outlet fluid temperatures were monitored using two different sensor systems during the experiment. 7 s time averaged data used in data analysis for this study was collected from temperature sensing cabling installed inside the BHEsat the top of the borehole/wellhead, whilst the inlet and outlet circulation flow temperature was also monitored using temperature probes (BMS) located in surface

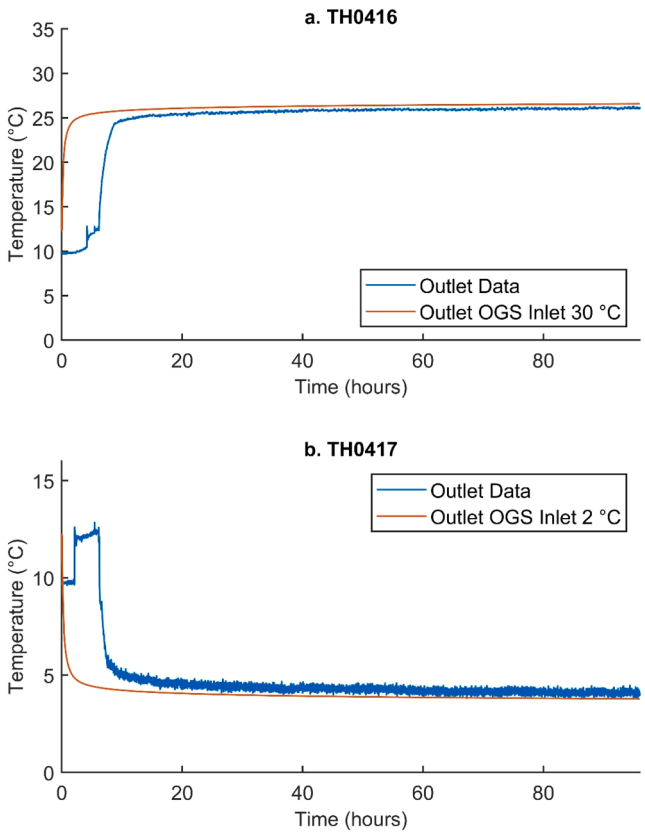

Fig. 14. Outlet temperatures for the modelled and experimental data comparing constant inlet temperature and that recorded during the experiment for BHEs (a) TH0416 and (b) TH0417.

pipework approximately 2 m from the wellheads. The BMS is accurate to 0.2 °C, whilst the temperature sensing at the wellhead is accurate to within 0.01 °C (according to user manuals/specifications). This means that the fluid temperature measured in the BMS does vary in comparison to that measured at the wellhead, with both data sources recorded in Fig. 16 (with temperature sensing at the wellhead labelled WH). Hot and cold circuit flow temperatures were regulated using separate temperature sensors located at the output of the heater unit and in the cold circuit buffer tank, respectively.

It can be observed that for the heat injection boreholes (Fig. 16a,d) there is minimal discrepancy between both sensor systems recorded data. The wellhead temperature is less variable, having a reduced amplitude and increased wavelength in comparison to BMS data. This may be due to different dwell time and frequency of the well head temperature sensing and BMS monitoring systems (7 s dwell time for the well head temperature sensing data and 1 min frequency versus ~no dwell and 1 min frequency for the BMS). Interestingly, a greater difference is observed in the heat extraction boreholes (Fig. 16b,c), with the BMS underpredicting both the inlet and outlet temperatures into the ground by up to 1.5 °C. The reason for this is not yet clear, possible causes include greater heat gain in the surface pipework between the BMS sensor and the wellhead, or issues with the BMS temperature sensor performance or setpoint programming.

4.2. Comparison between thermal performance test, core and numerical models

Numerical models and core measurements were compared to the estimated thermal conductivity from the TPT. Estimated effective thermal conductivity from TPT (2.43–3.65 W/mK) was within the range from measured saturated core (shown in Table 4 to range from 2.11–4 W/mK). The values in Table 4 were taken from core plugs from intervals of 33.61 m to 80.34 m for borehole (TH0424 – see Fig. 2 for map of borehole localities). These values lie directly within the range of the TPT for each borehole, providing some confidence that the estimated thermal properties are reasonable from the TPT. Further thermal conductivity measurements have also been taken in unsaturated rock sample from borehole TH0424 by Bremaud et al. (2025), and these range between 1.6 and 2.99 W/mK which also sits within the range expected from TPT analysis. Past literature has indicated that it is not uncommon for core to show strong variability and typically lower thermal conductivity to TRTs. This is because core samples may represent a range of geological features, groundwater can impact effective thermal conductivity values and in situ thermal conductivity is unlikely to agree with rock core data directly (Ramstad et al., 2009; Liebel et al., 2010). For instance, in Oslo, Norway, TRTs exhibit higher effective thermal conductivities due to groundwater associated to flow in karsts and fractures, which can give an increase in values by 23 % in comparison to core (Ramstad et al., 2009). The Sherwood Sandstone Group observed in this study is subject to fracturing and could explain the variations in measured effective thermal conductivity (Bowes et al., 2023).

However, there were more discrepancies when using numerical modelling to simulate the test. It was observed that there was a good fit between measured outlet fluid temperature data from the heat injection TPTs and that generated by OGS. In contrast, the heat extraction TPTs had a poorer alignment to forward modelling using OGS with it appearing ground thermal conductivities would be closer to 4 W/mK. This indicates that the TPT for the cold side could underestimate ground properties based upon numerical modelling results, although this could be due to the greater oscillatory behaviour observed in the data caused by the cycling of the chiller, the fact that the lower thermal conductivity cementitious grout is incorporated in the effective thermal conductivity value, or as others have suggested, the method of estimating TPTs may depart from the true data as it ignores changes in temperature between the borehole wall and fluid (Beier, 2021). There is also further ambiguity over the grout which could be greater (or less than) the 2 W/mK value inputted into the numerical model, which is listed on the manufacturer's website as the lowest possible value after mixing and setting in the borehole (GEOTHERM-X, 2025).

Parametric testing with OGS software demonstrated that variations in grout thermal conductivity, rock thermal conductivity, flow rate, and the presence of oscillatory data can all influence the modelled outlet temperature. In this study, numerical modelling suggests that the accuracy of estimating effective ground thermal conductivity was most affected by experimental oscillations, fluctuations in flow rate, and uncertainty in grout thermal conductivity measurements. It should also be noted the effects of free or forced convection within the aquifer were not considered in OGS and could impact results during numerical modelling.

Furthermore, the difference in effective thermal conductivity estimations could also be linked to the difference in inlet temperature for experiments and thus, the heat load imposed. The heat extraction boreholes rates were proximal to the typical lower limit of the 30 to 80 W/m recommended by Raymond et al. (2011). It highlights the practical difficulties of performing TPTs using chillers in contrast to TRTs which may impact the ability to determine accurate ground properties. They can reduce the rate of heat transfer and thermal pertubation into the surrounding rock meaning the test determines thermal conductivity values more influenced by the grout, and they may have greater cyclical behaviour impacting the ability to maintain a constant inlet temperature. Additionally, the higher thermal conductivities predicted by the numerical models of 4 W/mK could also indicate the TPTs are impacted from groundwater flow from transmissive fracture zones within the Chester Formation (Bowes et al., 2023). Others have also noted that heat extraction TPTs and TRTs provide lower thermal conductivity estimates as the natural convective effect in the ground can enhance the heat transfer effect in heat injection mode, thus increasing effective thermal conductivity estimates by up to 15 % (Witte, 2001; Jia et al., 2019). This

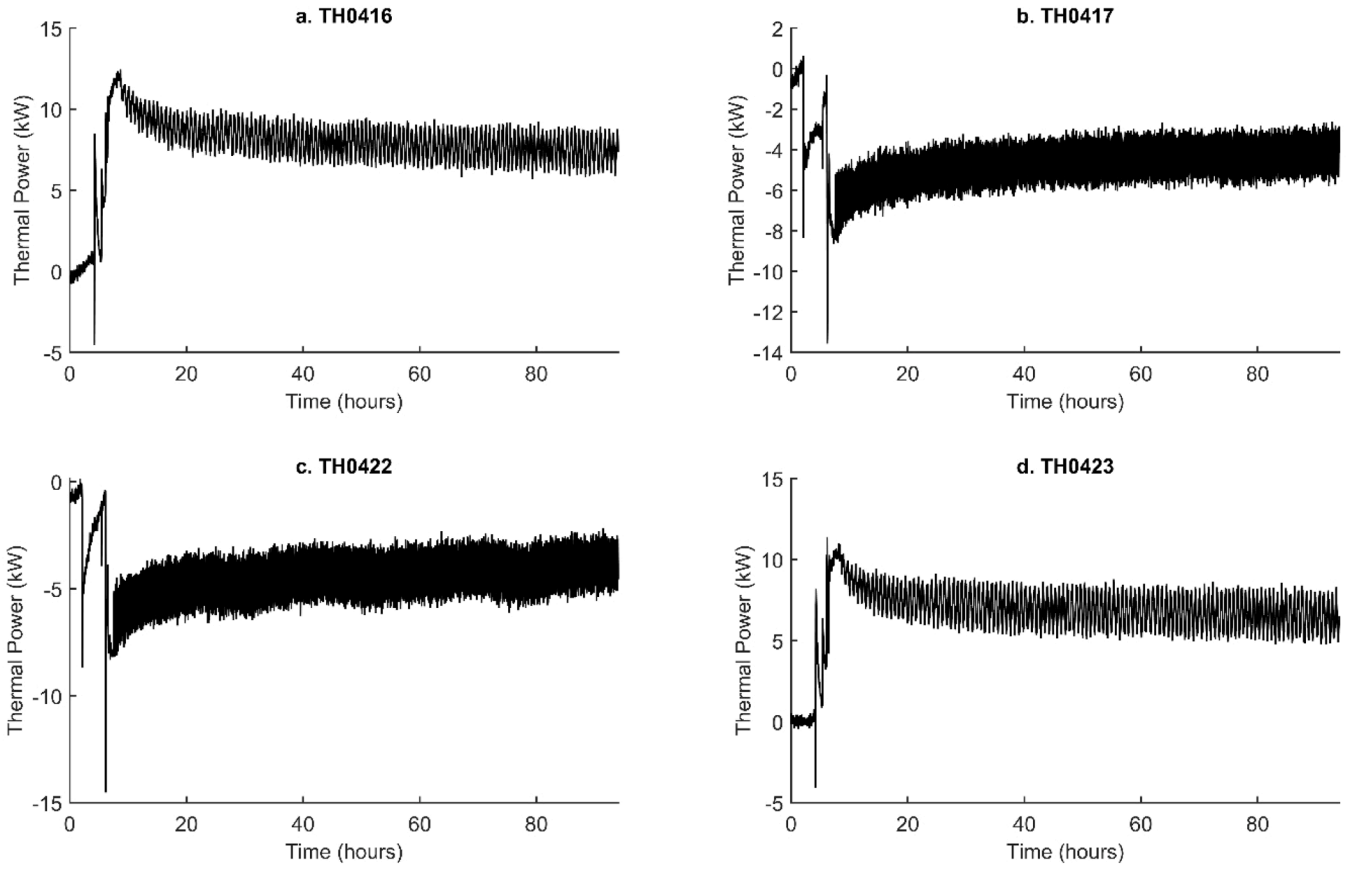

Fig. 15. Calculated thermal power for the duration of the experiment for BHEs a) TH0416, b) TH0417, c) TH0422, and d) TH0423.

can lead to bias in the results, and it could be better to design the system by using (i) seasonal planning if heating and cooling are both being considered using different effective thermal conductivity values from respective heat injection and extraction tests, or (ii) use an averaged thermal conductivity value from heat extraction and injection TPTs during system design.

To improve the quality of the test and reduce the potential for discrepancy to occur from the experimental set up, future tests should minimise the impact of oscillations of chillers and heaters. This could be achieved through using/reconfiguring the buffer tank or water tank and its control strategy to ensure a near constant outlet temperature is sustained to the BHEs. When evaluating the impact of engineering parameter future work could also test the grout thermal conductivity mix to better constrain the numerical models.

4.3. Study limitations

A key limitation of this experiment is that the UK Geoenergy Observatory heaters and chiller used introduce a significant amount of noise to the data set. A variation in amplitude of the wellhead measured temperature occurred up to ~0.8 °C either side of the set points. This results in a fluctuating inlet temperature which may lead to errors in determining the thermal conductivity estimates and far higher discrepancy of the data, which resulted in poor R^2 values ranging between 0.06 and 0.12. There were further experimental issues – the heat extraction mode TPTs failed to reach the set point of 1 °C at the wellhead and oscillated around 2 °C (see Fig. 17). It could be that there was some heat gained within the pipes linking the chiller and wellhead with air temperature typically greater than the set point for the duration of the experiment, or the heat was gained from the circulation pump. To fully understand the validity of the TPTs a TRT would also have been useful to compare the accuracy of results, and future work should investigate this further.

Practically, there are some advantages and disadvantages using TPTs in comparison to TRTs. TPTs can be more beneficial to system design by providing both in-situ parameter determination and also the thermal capacity of the system. However, TPTs are limited in the fact that it can be difficult to maintain the constant inlet temperature due to cycling of chillers and heaters. In contrast, TRTs may have more stability when maintaining a constant power; however, even using this method there can be fluctuations in power output. Furthermore, it has been envisioned that TPTs can be used for shorter tests in comparison to TRTs (Choi et al., 2019); however, this appears to not be possible if noise is introduced during testing. It was shown that this can lead to potential erroneous in-situ thermal properties estimation.

It would also be useful for heat extraction TPTs to be used when determining effective thermal conductivity and thermal capacity values for BHEs that will be used for supplying building heat (i.e., without thermal energy storage), and vice versa (i.e., heat injection TPTs for BHEs used for thermal energy storage). This will enable the thermal response of the ground to be obtained under operational conditions similar to that being used in long-term development. Further work should focus on clarifying the extent of the impact of noise on TPTs to determine if heat extraction TPTs can provide similar estimates to heat injection TPTs.

5. Conclusions

This study records what is believed to be one of the first TPTs documented in a UK setting, exploring a novel test of both heat injection and heat extraction modes. The effective thermal conductivity values generated from TPTs were tested in comparison to OGS software, utilising forward modelling of each TPT, with discrepancy typically <1 °C for the duration of the simulation. However, for the heat extraction TPTs

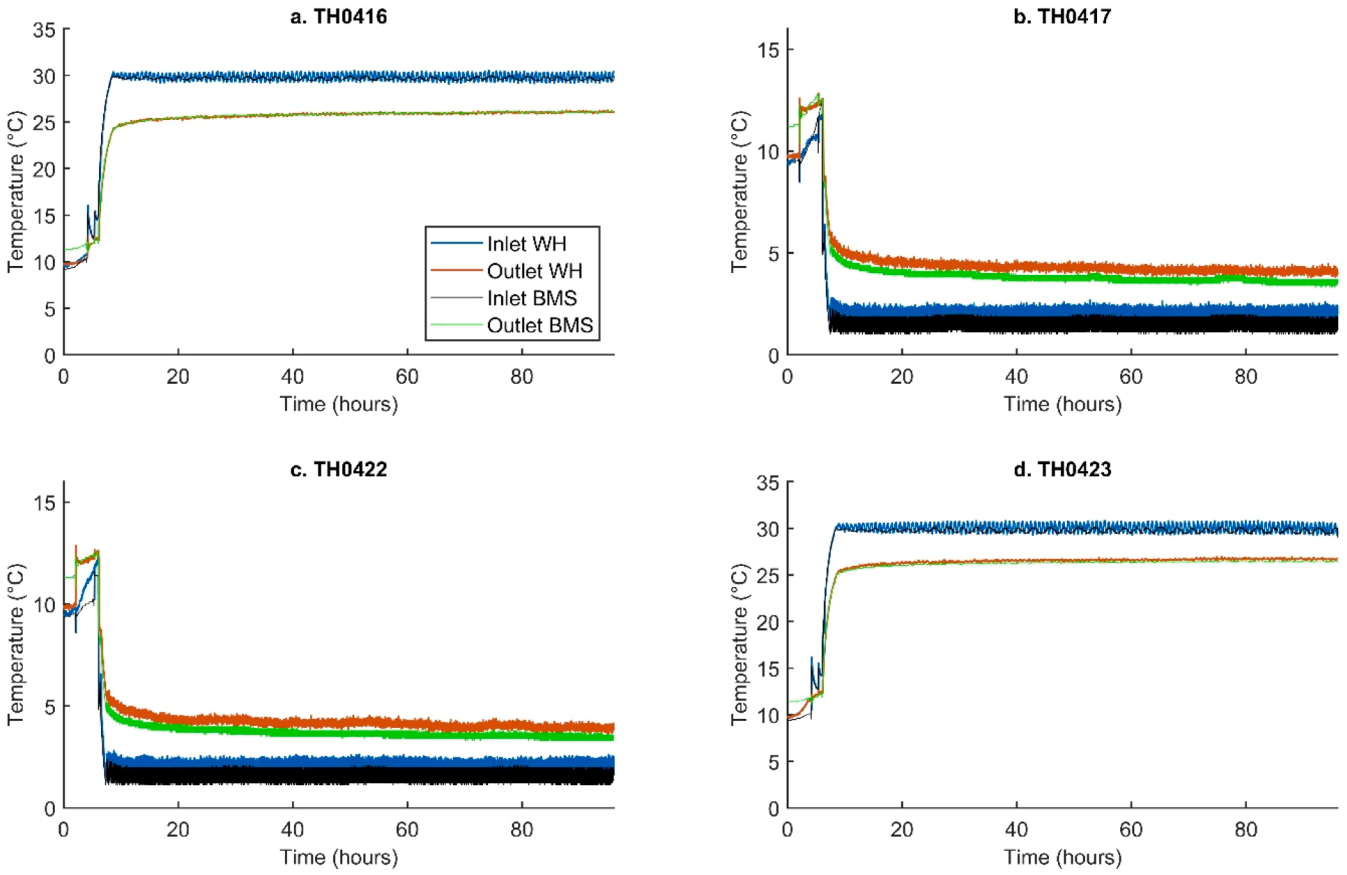

Fig. 16. Inlet and outlet temperatures measured on the building management system (BMS) and at the wellhead for the duration of the experiment for BHEs a) TH0416, b) TH0417, c) TH0422, and d) TH0423.

Table 4
Calculated average thermal conductivity values from borehole TH0424 at each depth (derived from the TH0424 final data pack - Contains NERC materials ©NERC 2024 - UKGEOS Cheshire Project Team, 2023).

Depth (m)	Average Thermal Conductivity (W/mK)
33.61	2.11
41.25	3.65
41.29	3.35
64.43	3.63
64.5	3.56
74.41	4
74.48	3.51
80.28	3.68
80.34	3.43

this resulted in an apparent underestimation of thermal conductivity values. Similarly, TPTs produced estimates of thermal conductivity within the range measured from core samples. The key findings of the test were:

1. TPTs can be used to determine the in-situ ground properties and in this study, they were used to determine an effective thermal conductivity of the ground to be between 2.43 and 3.65 W/mK.
2. Heat extraction TPTs appear to give under-estimations of the effective thermal conductivity, although this appears to be due to either i) the cycling of the chiller around the required inlet temperature, thereby distorting the data, or ii) as suggested by other authors this could also be due to the impact of natural convection of water bearing sediments leading to enhanced values of effective thermal conductivity in heat injection mode (Witte, 2001; Jia et al., 2019). This is particularly relevant as the Sherwood Sandstone Group is a known water bearing aquifer in the region.
3. There were significant practical issues during the test. Noise caused by cycling of the chiller and heater attempting to reach the set temperature point can introduce oscillations that can impact the experiment's accuracy, hence affecting its capability to be used as a data set for parameter determination. It may also result in erroneous values of effective thermal conductivity estimates at short time scales. In this experiment, the level of noise created fluctuations in inlet temperature over a ~1.5 °C interval. Further configuration of a water tank in the system to store the water at a stable temperature could help to minimise such fluctuations and improve the results (e.g., Aydin et al., 2019, 2024).
4. TPTs could serve a dual function: (i) to determine the in-situ thermal parameters in the subsurface and ii) to be used to determine the maximum likely thermal capacity of a GSHP system. For instance, at the end of the experiment for the heat extraction scenario the specific heat rates were recorded as ~40 W/m and ~38 W/m for boreholes TH0417 and TH0422, respectively. This could thus be used in further calculations for the system longevity when extracting heat. Similarly, for the heat injection boreholes specific heat rates of ~73 W/m and ~69 W/m were calculated for boreholes TH0416 and TH0423, respectively. This is essential for determining the capacity for

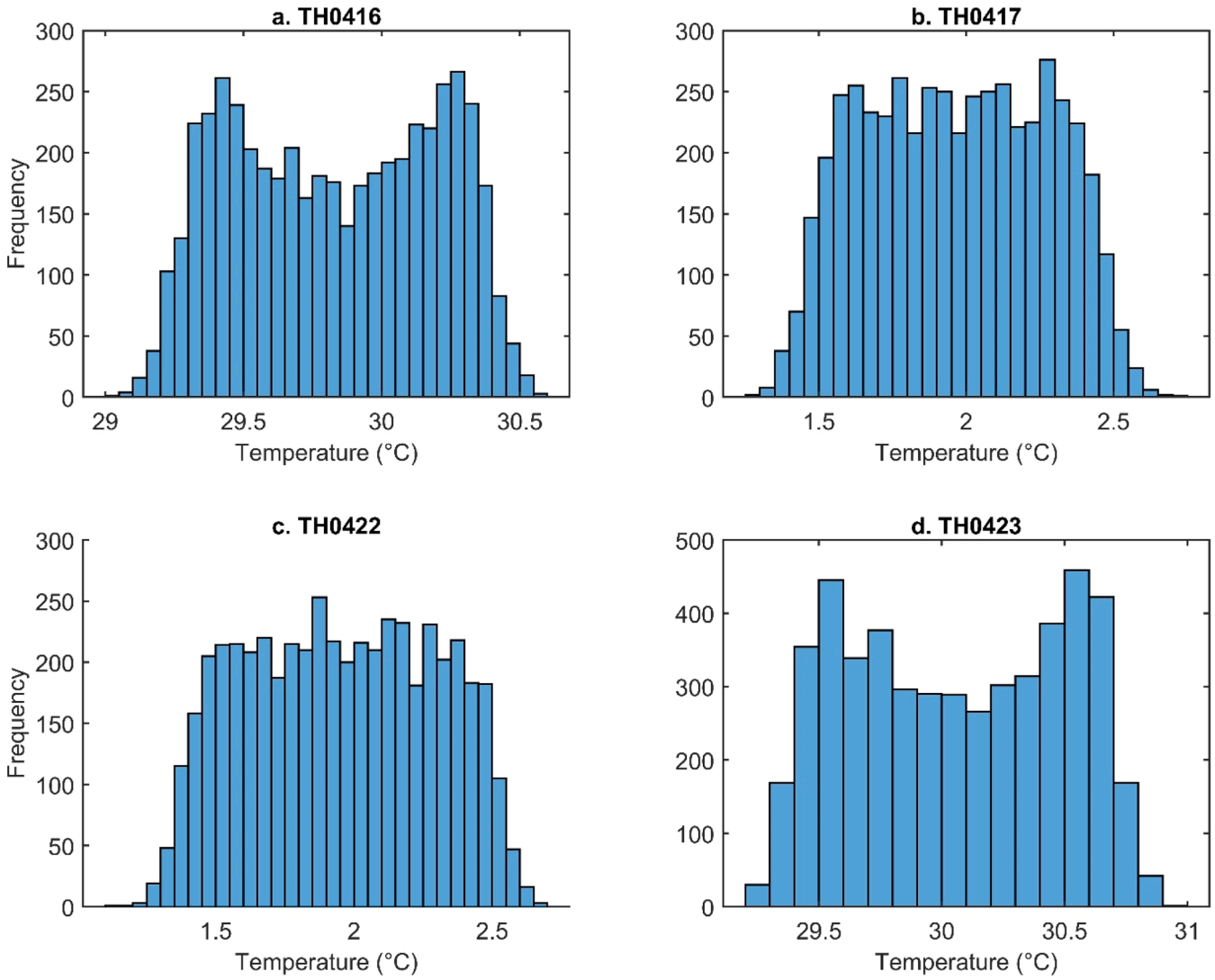

Fig. 17. Fluctuations in temperature recordings of the inlet temperature taken between 9 h and 94 h.

injecting heat either rejected as a cooling load or for borehole thermal energy storage.

CRediT authorship contribution statement

Christopher S. Brown: Writing – review & editing, Writing – original draft, Software, Project administration, Methodology, Investigation, Funding acquisition, Formal analysis, Data curation, Conceptualization. **Isa Kolo:** Writing – review & editing, Writing – original draft, Software, Investigation, Funding acquisition, Formal analysis. **Gioia Falcone:** Writing – review & editing, Funding acquisition. **Daniel Friedrich:** Writing – review & editing, Funding acquisition. **Sean M. Watson:** Writing – review & editing, Funding acquisition.

Declaration of competing interest

The authors declare the following financial interests/personal relationships which may be considered as potential competing interests:

Christopher Simon Brown reports financial support was provided by Engineering and Physical Sciences Research Council. If there are other authors, they declare that they have no known competing financial interests or personal relationships that could have appeared to influence the work reported in this paper.

Acknowledgments

The authors would like to acknowledge the support from EPSRC, grant reference EP/Z533129/1 - REnewable Energy access for Future UK Net-Zero Cooling (Reef-UKC). They would also like to thank Andres Gonzalez Quiros and Mylene Receveur for their constructive comments during an internal review. They would also like to thank 5 anonymous reviewers and the editor for constructive comments during the review process. For the purpose of open access, the author has applied a Creative Commons Attribution (CC BY) licence to any Author Accepted Manuscript version arising. Dr Isa Kolo was also supported by the Centre for Net Zero High Density Buildings for this work, which is funded by the UK Research and Innovation 'Building a Green Future' strategic theme (UKRI238).

Data availability

The authors do not have permission to share data.

References

Abesser, C., Gonzalez Quiros, A., Curtis, R., Raine, R., Claridge, H., 2023. Geothermal energy use, country update for United Kingdom. In: Proceedings of the World Geothermal Congress. Beijing, China, p. 2023. https://www.worldgeothermal.org/pdf/IGAstandard/WGC/2023//1720.pdf.

Angelotti, A., Ly, F., Zille, A., 2018. On the applicability of the moving line source theory to thermal response test under groundwater flow: considerations from real case studies. Geotherm. Energy 6, 1–17.
Attri, S.D., Heeg, E., Yilmaz, M., Tinjum, J.M., Fratta, D. and Hart, D., 2023. Long-term temperature monitoring of a campus-scale geothermal exchange field using a Fiber-optic sensing array.
Aydin, M., Onur, M., Sisman, A., 2017. A new method for constant temperature thermal response tests. In: Proceedings of the *42th Workshop on Geothermal Reservoir Engineering, Standford, California*, pp. 13–16.
Aydin, M., Onur, M., Sisman, A., 2019. A new method for analysis of constant-temperature thermal response tests. Geothermics 78, 1–8.
Aydin, M., Dolcek, A.O., Onur, M., Sisman, A., 2024. Flow-controlled thermal response test and its comparison with the conventional test methods. Geothermics 120, 103011.
Banks, D., Withers, J., Freeborn, R., 2009. An overview of the results of in-situ thermal response testing in the UK. In: Proceedings of the *11th International Conference on Thermal Energy Storage–Effstock*.
Banks, D., Withers, J.G., Cashmore, G., Dimelow, C., 2013. An overview of the results of 61 in situ thermal response tests in the UK. Quart. J. Eng. Geol. Hydrogeol. 46 (3), 281–291.
Banks, D., Brown, C.S., Kolo, I., Falcone, G., 2024. Generic modelling to develop thermal yield nomograms for coaxial deep borehole heat exchangers (DBHEs). Quart. J. Eng. Geol. Hydrogeol. 57 (3) qjegh2023-162.
Beier, R.A., 2020. Thermal response tests on deep borehole heat exchangers with geothermal gradient. Appl. Therm. Eng. 178, 115447.
Beier, R.A., 2021. Analysis of thermal response tests on boreholes with controlled inlet temperature versus controlled heat input rate. Geothermics 94, 102099.
Beier, R.A., 2024. Thermal response tests on boreholes in multi-layered ground with geothermal gradient. Appl. Therm. Eng. 253, 123848.
BGS GeoIndex Onshore, 2025. Accessed on 07/04/2025: https://mapapps2.bgs.ac.uk/geoindex/home.html?layer=BGSBoreholes&_ga=2.86140891.278559725.1744017146-384329554.1744017146.
Bowes, M., Crewdson, E., Elsome, J. and Spence, M., 2023. UK geoenergy observatories Cheshire: hydraulic testing of TH0424 technical summary.
Bremaud, M., Burnside, N., Shipton, Z., Bossennec, C., Fuchs, S. and Deon, F., 2025. Bridging surface and subsurface: comparative analysis of outcrop and core samples from the Chester Formation for geothermal exploration. Preprint, Available at SSRN 5177375.
Brown, C.S., 2023. Revisiting the deep geothermal potential of the Cheshire Basin, UK. Energies 16 (3), 1410.
Brown, C.S., Kolo, I., Falcone, G., Banks, D., 2023a. Investigating scalability of deep borehole heat exchangers: numerical modelling of arrays with varied modes of operation. Renew. Energy 202, 442–452.
Brown, C.S., Kolo, I., Banks, D., Doran, H.R., Falcone, G., 2023b. Modelling Thermal Response Tests For Deep Coaxial Borehole Heat Exchangers. World Geothermal Congress, Beijing, China.
Brown, C.S., Doran, H., Kolo, I., Banks, D., Falcone, G., 2023c. Investigating the influence of groundwater flow and charge cycle duration on deep borehole heat exchangers for heat extraction and borehole thermal energy storage. Energies 16 (6), 2677.
Brown, C.S., Kolo, I., Banks, D., Falcone, G., 2024. Comparison of the thermal and hydraulic performance of single U-tube, double U-tube and coaxial medium-to-deep borehole heat exchangers. Geothermics 117, 102888.
Cai, W., Wang, F., Jiang, J., Wang, Z., Liu, J., Chen, C., 2022. Long-term performance evaluation and economic analysis for deep borehole heat exchanger heating system in Weihe basin. Front. Earth Sci. 10, 806416.
Cai, W., Wang, F., Chen, S., Chen, C., Liu, J., Deng, J., Kolditz, O., Shao, H., 2021. Analysis of heat extraction performance and long-term sustainability for multiple deep borehole heat exchanger array: a project-based study. Appl. Energy 289, 116590.
Carslaw, H.S., Jaeger, J.C., 1959. Conduction of Heat in Solids (No. 536.23). Clarendon Press.
Charlton, T.S., Rouainia, M., 2025. Polynomial chaos-based uncertainty quantification of the performance of a closed loop deep geothermal borehole. Geothermics 129, 103271.
Chen, C., Shao, H., Naumov, D., Kong, Y., Tu, K., Kolditz, O., 2019. Numerical investigation on the performance, sustainability, and efficiency of the deep borehole heat exchanger system for building heating. Geotherm. Energy 7, 1–26.
Chen, S., Cai, W., Witte, F., Wang, X., Wang, F., Kolditz, O., Shao, H., 2021. Long-term thermal imbalance in large borehole heat exchangers array–A numerical study based on the Leicester project. Energy Build. 231, 110518.
Choi, W., Ooka, R., 2015. Interpretation of disturbed data in thermal response tests using the infinite line source model and numerical parameter estimation method. Appl. Energy 148, 476–488.
Choi, W., Kikumoto, H., Ooka, R., 2019. Critical comparison between thermal performance test (TPT) and thermal response test (TRT): differences in heat transfer process and extractable information. Energy Convers. Manag. 199, 111967.
Downing, R.A., Gray, D.A., 1986. Geothermal energy – the potential in the United Kingdom. British Geological Survey. HMSO, London.
Eklöf, C. and Gehlin, S., 1996. TED-a mobile equipment for thermal response test: testing and evaluation.
Esen, H., Inalli, M., 2009. In-situ thermal response test for ground source heat pump system in Elazığ, Turkey. Energy Build. 41 (4), 395–401.
Gehlin, S., 2002. *Thermal response test: method development and evaluation* (Doctoral dissertation, Luleå tekniska universitet).
GEOTHERM-X, 2025. GEOTHERM-X GR geothermal injection mortar, accessed on 07/04/2025: https://www.euroquartz.be/producten/geotherm-x-gr/?lang=en.
Gonzalez Quiros, A., Monaghan, A. and Robinson, S., 2024. 2023 United Kingdom country report. IEA Geothermal, October 2024.
Hart, D.J., Tinjum, J.M., Fratta, D., Thomas, L.K., Carew, E.L., 2022. Radiators or reservoirs: heat budgets in district-scale ground-source geothermal exchange fields. In: Proceedings of the 47th Workshop on Geothermal Reservoir Engineering. Stanford University.
Heim, E., Stoffel, P., Müller, D., Klitzsch, N., 2024. Six years of high-resolution monitoring data of 40 borehole heat exchangers. Sci. Data 11 (1), 1334.
HM Government, 2023. Heat pump investment Roadmap. Leading the way to net zero, April 2023. Accessed on 20/02/2025: https://assets.publishing.service.gov.uk/government/uploads/system/uploads/attachment_data/file/1166439/heat-pumps-investment-roadmap.pdf.
Ingersoll, L.R., Zobel, O.J., Ingersoll, A.C., 1954. Heat Conduction, With Engineering, Geological and Other Applications, 1954. University of Wisconsin Press, p. 325.
Jackson, T., 2012. Geothermal potential in Great Britain and Northern Ireland. Sinclair Knight Merz: Sydney. NSW, Australia.
Jia, J., Lee, W.L., Cheng, Y., 2019. Field demonstration of a first constant-temperature thermal response test with both heat injection and extraction for ground source heat pump systems. Appl. Energy 249, 79–86.
Kolditz, O., Bauer, S., Bilke, L., Böttcher, N., Delfs, J.O., Fischer, T., Görke, U.J., Kalbacher, T., Kosakowski, G., McDermott, C.I., Park, C.H., 2012. OpenGeoSys: an open-source initiative for numerical simulation of thermo-hydro-mechanical/chemical (THM/C) processes in porous media. Environ. Earth Sci. 67, 589–599.
Kolo, I., Brown, C.S., Falcone, G., Banks, D., 2023. Repurposing a geothermal exploration well as a deep borehole heat exchanger: understanding long-term effects of lithological layering, flow direction, and circulation flow rate. Sustainability 15 (5), 4140.
Kolo, I., Brown, C.S., Watson, S., Lyden, A., Friedrich, D., Falcone, G., 2025. Surface–subsurface modelling of seasonal borehole thermal energy storage for a university building. J. Energy Storage 113, 115598.
Li, M., Tan, Y., Wu, Y., Wang, Q., Li, Y., 2024. New algorithm for estimating parameters from interrupted thermal response tests of ground heat exchangers. Appl. Therm. Eng. 239, 122088.
Liebel, H.T., Huber, K., Frengstad, B.S., Kalskin Ramstad, R., Brattli, B., 2010. Rock core samples cannot replace thermal response tests—A statistical comparison based on thermal conductivity data from the Oslo Region (Norway). In: Proceedings of the Renewable Energy Conference, pp. 145–154.
Maghrabie, H.M., Abdeltwab, M.M., Tawfik, M.H.M., 2023. Ground-source heat pumps (GSHPs): materials, models, applications, and sustainability. Energy Build. 299, 113560.
McDaniel, A., Tinjum, J., Hart, D.J., Lin, Y.F., Stumpf, A., Thomas, L., 2018. Distributed thermal response test to analyze thermal properties in heterogeneous lithology. Geothermics 76, 116–124.
Oh, H.R., Baek, J.Y., Park, B.H., Kim, S.K., Lee, K.K., 2025. Influence of borehole characteristics on thermal response test analysis using analytical models. Appl. Therm. Eng. 268, 125892.
Priarone, A., Fossa, M., 2015. Modelling the ground volume for numerically generating single borehole heat exchanger response factors according to the cylindrical source approach. Geothermics 58, 32–38.
Rainieri, S., Bozzoli, F., Pagliarini, G., 2011. Modeling approaches applied to the thermal response test: a critical review of the literature. HVAC&R Res. 17 (6), 977–990.
Ramstad, R.K., Brattli, B., Liebel, H.T., Huber, K. and Frengstad, B., 2009. Thermogeology in the Oslo region and Kristiansand-results from thermal response tests (TRT) with and without artificially induced groundwater flow.
Raymond, J., Robert, G., Therrien, R., Gosselin, L., 2010. A novel thermal response test using heating cables. In: Proceedings of the World Geothermal Congress. Bali, Indonesia, pp. 1–8.
Raymond, J., Therrien, R., Gosselin, L., Lefebvre, R., 2011. A review of thermal response test analysis using pumping test concepts. Groundwater 49 (6), 932–945.
Raymond, J., Lamarche, L., Malo, M., 2015. Field demonstration of a first thermal response test with a low power source. Appl. Energy 147, 30–39.
Raymond, J., 2018. Colloquium 2016: assessment of subsurface thermal conductivity for geothermal applications. Can. Geotech. J. 55 (9), 1209–1229.
Receveur, M., McDermott, C.I., Fraser-Harris, A., Gilfillan, S., Watson, I., 2024. Quantifying vertical borehole heat exchanger sustainability from a geothermal resource perspective in the UK. Geoenergy 2 (1) geoenergy2023-040.
Rollin, K.E., Kirby, G.A., Rowley, W.J., 1995. Atlas of Geothermal Resources in Europe: UK Revision. British Geological Survey, Regional Geophysics Group.
Seib, L., Krusemark, M., Lehr, C., Ohagen, M., Pham, H., Schedel, M., Welsch, B., Sass, I., 2025. Distributed Geothermal Response Test on a 750 m Deep Borehole Thermal Energy Storage System. Applied Thermal Engineering, 126322.
Shao, H., Hein, P., Sachse, A., Kolditz, O., 2016. Geoenergy Modeling II: Shallow Geothermal Systems. Springer International Publishing, Berlin/Heidelberg, Germany.
Signorelli, S., Bassetti, S., Pahud, D., Kohl, T., 2007. Numerical evaluation of thermal response tests. Geothermics 36 (2), 141–166.
Spitler, J.D., Gehlin, S.E., 2015. Thermal response testing for ground source heat pump systems—An historical review. Renew. Sustain. Energy Rev. 50, 1125–1137.
UKGEOS Cheshire Project Team, 2023. UKGEOS Cheshire - TH0424 Final Borehole Information Pack. NERC EDS National Geoscience Data Centre. (Dataset). https://doi.org/10.5285/badff3b9-8bc8-4897-b324-7f4653fdd214.
Viesi, D., Galgaro, A., Zanetti, A., Visintainer, P., Crema, L., 2018. Experimental geothermal monitoring assessing the underground sustainability of GSHP borehole heat exchangers in a protected hydrothermal area: the case Study of Ponte Arche (Italian Alps). Geothermics 75, 192–207.

Wagner, V., Bayer, P., Kübert, M., Blum, P., 2012. Numerical sensitivity study of thermal response tests. Renew. Energy 41, 245–253.
Waples, D.W., Waples, J.S., 2004. A review and evaluation of specific heat capacities of rocks, minerals, and subsurface fluids. Part 1: minerals and nonporous rocks. Nat. Resour. Res. 13, 97–122.
Wang, C., Jiang, T., Zhou, X., Guo, Y., Huang, X., Lu, J., 2025. Estimation method of soil thermal conductivity distribution of coaxial vertical borehole heat exchanger based on distributed thermal response test. Renew. Energy 238, 121954.
Wilke, S., Menberg, K., Steger, H., Blum, P., 2020. Advanced thermal response tests: a review. Renew. Sustain. Energy Rev. 119, 109575.
Witte, H.J.L., 2001, October. Geothermal response tests with heat extraction and heat injection: examples of application in research and design of geothermal ground heat exchangers. In *Workshop Geothermal Response Tests* (pp. 48–63).
Yu, X., Zhang, Y., Deng, N., Ma, H., Dong, S., 2016. Thermal response test for ground source heat pump based on constant temperature and heat-flux methods. Appl. Therm. Eng. 93, 678–682.
Zarrella, A., Emmi, G., Graci, S., De Carli, M., Cultrera, M., Santa, G.D., Galgaro, A., Bertermann, D., Müller, J., Pockelé, L., Mezzasalma, G., 2017. Thermal response testing results of different types of borehole heat exchangers: an analysis and comparison of interpretation methods. Energies 10 (6), 801.
Zhang, C., Guo, Z., Liu, Y., Cong, X., Peng, D., 2014. A review on thermal response test of ground-coupled heat pump systems. Renew. Sustain. Energy Rev. 40, 851–867.
Zhang, Y., Hao, S., Yu, Z., Fang, J., Zhang, J., Yu, X., 2018. Comparison of test methods for shallow layered rock thermal conductivity between in situ distributed thermal response tests and laboratory test based on drilling in northeast China. Energy Build. 173, 634–648.